AN ABSTRACT OF THE THESIS OF

J. Peter Weidenheim for the degree of Master of Science

in Department of Geology presented on 30 May 1980

Title: The Petrography, Structure, and Stratigraphy of Powell Buttes, Crook County, Central Oregon

Abstract approved: Redacted for Privacy

Dr. Edward M. Taylor

Powell Buttes is a major topographic feature located in western Crook County, between Bend and Prineville in central Oregon, and represents a mid-Tertiary silicic volcanic center of probable John Day age. The rocks of Powell Buttes are sparsely porphyritic and include dacite, rhyodacite, basaltic andesite, and flowbanded rhyolite in the form of lava flows and domes.

A warm climate with lush vegetation and frequent ash falls is recorded by carbonized plant remains and ancient soil horizons in tuffaceous sediments. The ash falls were products of Plinean volcanic activity; Pelean-type eruptions produced numerous vitroclastic breccias and lapilli tuffs, some of which contain authigenic clinoptilolite. The deposits and their characteristics suggest that Powell Buttes represent a source area for some John Day air-fall and ash-flow tuffs. The mature topography exhibited by Powell Buttes indicates that erosional processes have been very active in the past. This implies that Powell Buttes contributed sediment to the nearby Pliocene Deschutes Formation.

Major oxide analyses of Powell Buttes rocks indicate a calc-alkaline suite when plotted on a Peacock diagram and Harker variation

diagrams of the major oxides. A plot of Na_2O to K_2O results in an inverse relationship similar to that demonstrated by Walker (1970) for ash-flow tuffs of Oregon, some of which are John Day in age.

A subducting plate has been postulated to have existed approximately 260 km (155 mi.) west of the study area during the mid-Tertiary (Atwater, 1970). Calc-alkaline volcanism has been associated with the subduction process and may be related to the silicic lavas exposed at Powell Buttes. Pitts (1979) mapped a major positive gravity anomaly at Powell Buttes and suggested that an olivine-gabbro residuum exists at depth. Other possibilites, however, should be considered because 1) the volume of rhyolite and dacite would require parental mafic and intermediate magmas that should be even more abundant than the silicic lavas, and 2) such residual rocks are not exposed in old, deeply eroded calc-alkaline belts.

A 7.4 km (4.4 mi.) long east-west normal fault, with the north side downthrown approximately 300 m (985 ft.), is delineated in the central area of Powell Buttes by a subtle, yet abrupt lithologic discontinuity of dacite to rhyolite.

The author has verified the occurrence of geothermal activity (Pg. 56) in the area adjacent to the northern part of Powell Buttes. Young silicic volcanic centers are usually associated with geothermal activity, but none exist in the region surrounding Powell Buttes.

THE PETROGRAPHY, STRUCTURE, AND STRATIGRAPHY OF POWELL BUTTES, CROOK COUNTY, CENTRAL OREGON

by

Jan Peter Weidenheim

A THESIS

submitted to

Oregon State University

in partial fulfillment of the requirements for the degree of

Master of Science

June 1981

APPROVED:

Redacted for Privacy

Professor of Geology in charge of major.

Redacted for Privacy

Chairman of the Department of Geology

Redacted for Privacy

Dean of Graduate School

Date thesis is presented: 30 May 1980

Typed by: J. Peter Weidenheim

ACKNOWLEDGEMENTS

The author would like to extend a special thanks to Dr. Edward M. Taylor for his time and invaluable suggestions provided during this study. The author also extends this appreciation to Dr. Harold E. Enlows for his assistance with the petrography and Dr. Keith F. Oles for critically reading the manuscript.

The Oregon Department of Geology and Mineral Industries provided a part of the author's financial support, for which he is most grateful.

Mr. and Mrs. Harold Weitgenant provided a base camp for the summer field work and some of the best "home cooking" in central Oregon, for which the author is especially indebted.

TABLE OF CONTENTS

LIST OF FIGURES

LIST OF PLATES

THE PETROGRAPHY, STRUCTURE, AND STRATIGRAPHY OF POWELL BUTTES, CROOK COUNTY, CENTRAL OREGON

INTRODUCTION

Powell Buttes is a major topographic feature located between Bend and Prineville in central Oregon. Silicic volcanic and volcaniclastic rocks in the form of volcanic domes, lava flows, air-fall tuffs, and ash-flow tuffs of probable John Day age predominate. The Buttes are significant geologically because they represent a possible source area for many of the middle Tertiary ash flows, air-fall tuffs, epiclastic volcanic sediments, and lava flows indigenous to the area.

Location and Accessibility

The area of this study is located in western Crook County, central Oregon (Figure 1). Approximately 65 km^2 were mapped, including all or parts of sections 29, 31-35, T. 15 S., R. 15 E.; section 36, T. 15 S., R. 14 E.; sections 1, 2, 10-15, 22-27, 35,36, T. 16 S., R. 14 E.; sections 2-11, 15-22, 29, 30, T. 16 S., R. 15 E. The project area is shown on the Powell Buttes 7.5' quadrangle (1962) and the Powell Buttes 15' quadrangle (1962).

U. S. Highway 126, a main east-west thoroughfare, crosses within 2.4 km of the northern boundary of the thesis area. The study area is traversed by many public and private improved and unimproved roads. Some of the roads have fallen into disuse and are traversable only by four-wheel-drive vehicles.

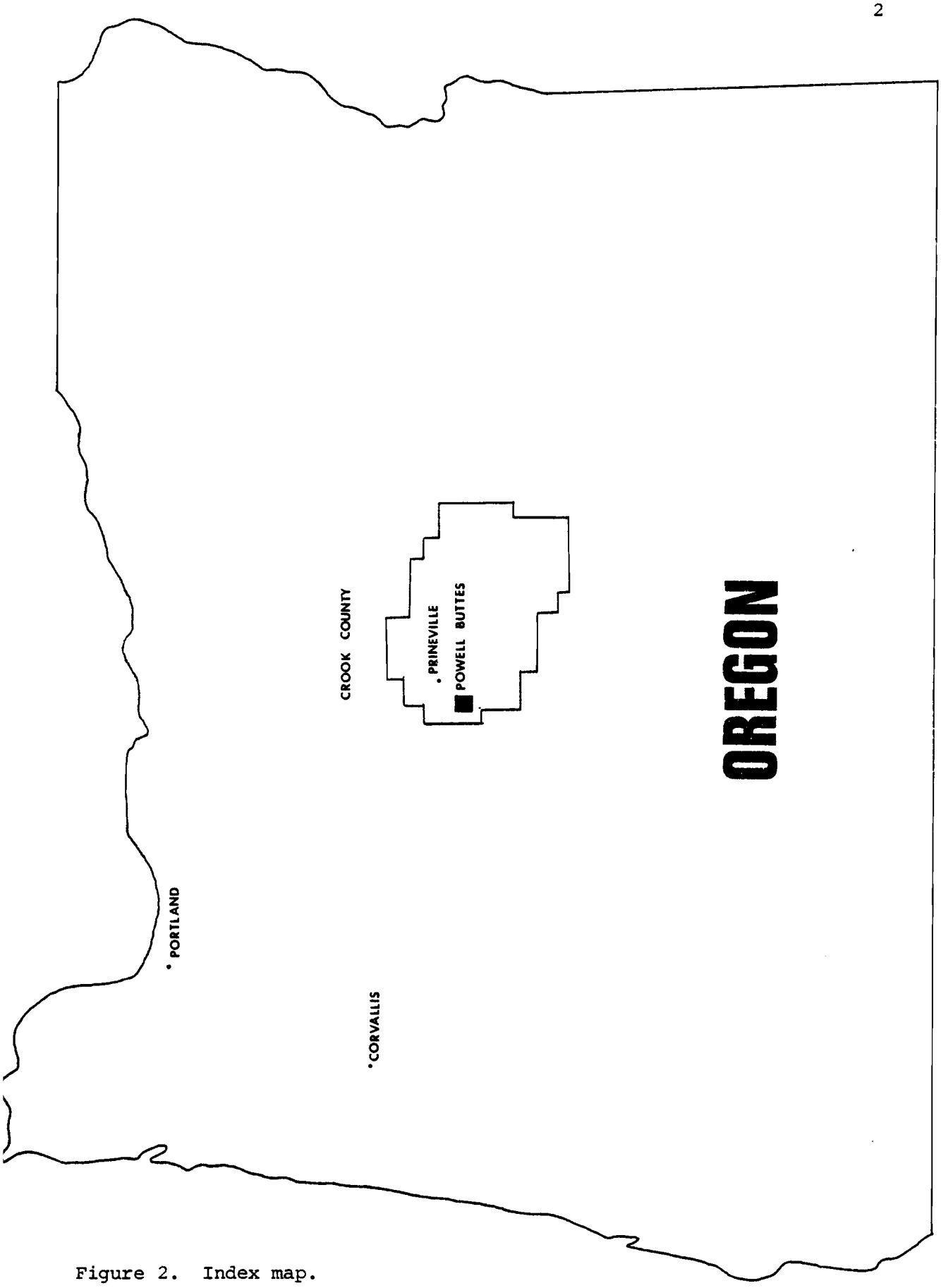

Figure 2. Index map.

Physiography and Climate

The project area is a maturely dissected silicic volcanic center of Tertiary age. Topography consists of prominent ridges of rhyolite lava separated by moderate to steep slopes and deep canyons. Elevations in the study area range from 967 m on U. S. 126 to 1568 m on top of Powell Buttes, with a relief of 601 m. The area includes many small-to-large rhyolitic domes.

A radial drainage pattern of many intermittent streams surrounds Powell Buttes. These streams are active only in the spring or during periods of unusually heavy rainfall. They drain westward to the Dry River and Central Oregon Canal; to the north, south, and east they debouch onto the surrounding plain.

Powell Buttes is approximately 48 km east of the central Cascades and within their rainshadow. Thus, the climate is semi-arid and the vegatation consists mainly of juniper, sage, and range grass. Some Ponderosa Pine trees are present at higher elevations on the Buttes. The semi-arid climate and sparse vegetation are contributing factors to the fairly good exposures of rock.

Purposes and Methods of Investigation

The principal purposes of this investigation were to construct a detailed geologic map of the study area and describe in detail the mineralogical and chemical composition of the rocks. An additonal objective was to contribute further knowledge concerning the origin and distribution of the John Day Formation in Oregon and aid in deciphering the mid-Oligocene to early Miocene tectonic history of the Pacific Northwest.

Ten weeks were spent in the field during the summer of 1979. Field data were recorded on the Powell Buttes quadrangle maps. Aerial photos at a scale of 1:62,500 were used to facilitate the mapping.

The colors of all fresh and altered rock samples were named in accordance with the Rock-Color Chart published by the Geological Society of America (Goddard, 1963). Attitudes of the beds were measured with a Brunton compass.

Approximately 300 rock specimens were collected and of these 55 were examined in thin-section to determine the petrographic characteristics of the rocks. Compositions of well developed plagioclase crystals were determined by the statistical method of Michel-Levy and by the extinction angles of Carlsbad-albite twins cut normal to (010) (Kerr, 1959).

Selected rock billets were also stained for alkali and plagioclase feldspar according to Laniz et al. (1964). The alkali feldspar was stained a bright-rusty-yellow and the plagioclase a grape-red by application of cobaltinitrite and amaranth dye solutions respectively. The staining also delineated in greater detail the flow-bands of the groundmass and minute embayments in the phenocrysts.

Whole-rock chemical analyses were performed on 12 samples considered representative of the mapped units. All samples were brought to an anhydrous condition before analysis. Weight percentages of SiO_2, FeO (total iron), TiO_2 CaO, K_2O, and Al_2O_3 were determined by X-ray fluorescence spectrophotometry, and Na_2O and MgO were determined by atomic absorption spectrophotometry. The analyses were performed by Ruth L. Lightfoot under the direction of Dr. E. M. Taylor, Department of Geology, Oregon State University.

Igneous rock nomenclature was based on weight percent increments of silica as proposed by Taylor (1978). Rocks with a SiO_2 content between 48 and 53 percent are classified as basalts, between 53 and 58 percent as basaltic andesites, 58 and 63 percent as andesites, between 63 and 68 percent as dacites, and those with more than 68 percent as rhyodacite. Rhyolites are defined as those rocks containing greater than 73 percent SiO_2 and greater than four percent K_2O. In the absence of chemical data, the IUGS classification (Streckeisen, 1979) of volcanic rocks was employed where petrographic data were available. Volcaniclastic rocks were named according to fisher (1961).

Regional Geology

The project area consists of a silicic Tertiary volcanic center which has been reported to be John Day in age (Swanson, 1969). In central Oregon, the John Day Formation lies unconformably on the Clarno Formation, a thick unit of andesitic lava flows and volcanic breccias (Figure 2), and is unconformably overlain by basalts of the Columbia River Group.

In the project area, the author has observed silicic domes, sparsely porphyritic rhyolite and dacite flows, and aphyric basaltic andesite and rhyodacite. Also present are tuffaceous epiclastic sediments, air-fall tuffs, vitroclastic lapilli tuffs, welded ash flows, and a volcanic conglomerate.

The structural pattern surrounding the thesis area consists of a few large- and small-scale northeast-southwest-trending anticlines and synclines. The Blue Mountain Anticline is approximately 8 km north of Powell Buttes and trends northeast-southwest for 270 km.

AGE		FORMATION	LITHOLOGY	AGE*
Quaternary	Pleisto-cene	Quaternary Deposits	Alluvium	
Tertiary	Pliocene	Deschutes	Fluvial Sandstone, Siltstones, Mudflows, Conglomerates, Tuffs, Basalt, Andesite, Ignimbrite	4.3 5.3 15.3
		Rattlesnake	Ignimbrite	6.41 6.56
	Late Miocene	Mascall	Fluvial Sandstones, Tuffs, Conglomerates, Ignimbrite	15.8
		Picture Gorge	Tholeiitic Basalt	14.7 15.4
	Early Miocene to Middle Oligocene	John Day	Tuffs, Ignimbrites, Rhyolite, Alkali Basalt, Trachyandesite, Quartz Latite	22 23.3 32.0
	Early Oligocene to Middle Eocene	Clarno	Basalt, Andesite, Tuffs, Ignimbrites, Rhyodacite, Dacite, Intrusive Rocks	36.5 48.9
Cretaceous	Albian Cenomanian	Hudspeth Gable Creek	Marine Mudstone, Graywacke, Conglomerate	
Permian		Metasediments	Glaucophane-Lawsonite Schist, Phyllite, Marble	

Figure 2. Regional stratigraphic column. Age date references: Hay (1962), Evernden and James (1964), Evernden et al. (1964), Walker et al. (1967), Davenport (1971), Walker et al. (1974), Enlows (1976), Laursen and Hammond (1978), Enlows (1980).
* Denotes age in millions of years.

The smaller east-west-trending Ochoco Anticline is approximately 38 km north-northeast of Powell Buttes. South of the Ochoco Anticline, and 40 km east of Powell Buttes, the Post Anticline trends northeast-southwest. Swanson (1968) suggests that two synclines parallel one another with an anticline between them southeast of Powell Buttes. Research by Rogers (1966) and Fisher (1967) indicates these structural complexities were produced during the middle Tertiary and are therefore not to be expected in younger undeformed rocks surrounding Powell Buttes.

Previous Work

I. John Day Formation

Marsh (1875) first named and described the John Day Formation from exposures along the John Day River between Clarno and Picture Gorge. Later, Merriam (1901a, b) provided the type description and Calkins (1902) first studied the petrography of the rocks in the region.

A later study by Hay (1962) delineated two mineralogic facies within the John Day Formation. Hay found clinoptilolite replacing vitric material in most claystones and tuffs of the lower part of the formation, which he designated the clinoptilolite facies. The upper part of the formation was designated the fresh glass facies since zeolite was absent.

Other studies by Peck (1964) and Oles and Enlows (1971) identified fluvial and lacustrine tuffs, epiclastic sandstone, conglomerate, ignimbrite, trachyandesite, dacite and rhyolite flows, and domes belonging to the John Day Formation.

Swanson and Robinson (1968) have observed that many of the John Day tuffs were erupted from vents near the 121st meridian and spread eastward into the John Day Basin, but that most of the lava flows are indigenous to their particular locality. Other authors including Waters (1954), Peck (1964), and Walker (1970) have suggested vents for small-to-moderate volume ash-flow tuffs that may be obscured by silicic volcanic piles, such as at Powell Buttes.

Some of the lapilli tuffs of the John Day Formation become increasingly abundant toward the Cascades and differ in composition from volcanic rocks of central Oregon, but are similar to contemporaneous pyroclastic rocks in the Cascade Range. This suggests that some of the John Day Formation was formed as ash was carried eastward by aeolian transport from vents in an ancestral Cascade Range (Calkins, 1902; Hodge, 1932; Coleman, 1949; Fisher and Wilcox, 1960; Taylor, 1960; Hay 1962, 1963; Peck, 1964; and Walker, 1970).

II. Powell Buttes

Russell (1905) compiled the first brief description of Powell Buttes in his preliminary report on the geology and water resources of western Oregon. According to Russell, Powell Buttes consists of a hard and resistant rhyolitic tuff in which the bedding is dintinct and steeply inclined to the southwest at 65° to 70°. Russell also noted a fine rich soil in the canyons to which he ascribed an aeolian origin. Ephemeral streams have transported much of this material to broad alluvial fans which extend onto the surrounding plain. Small hillside springs also surface at the heads of a few canyons.

Other authors including Wells and Peck (1961), and Swanson (1969) have described Powell Buttes as consisting of dacite and flowbanded rhyolite flows, domes, small near surface intrusive bodies, welded tuff, bedded tuff, and fine-grained fluviatile and lacustrine tuffaceous sedimentary rocks. Most of the rhyolite and dacite has been described as sparsely porphyritic with phenocrysts of chalky-white oligoclase, alkali feldspar, and quartz.

III. Deschutes Formation

The Deschutes Formation which surrounds Powell Buttes was originally described along the Deschutes River and designated the "Deschutes Sand" by Russell (1905). More recent descriptions of the Deschutes Formation describe it as a fluviatile and lacustrine conglomerate with thin-to-medium bedded semiconsolidated sandstone, tuff, siltstone, claystone, and coarse mudflow breccia, all of andesitic or dacitic composition.

The Deschutes Formation is synonomous with the Dalles Formation (Hodge, 1942) and the Madras Formation (Hodge, 1940; Williams, 1957; and Waters, 1968). Baldwin (1964) states that both Madras and Deschutes have been used for the same beds in the upper Deschutes River Valley. Baldwin notes that the name Dalles would have priority if the Madras and Deschutes are equivalent, but if not, it would seem that the name Deschutes would have priority. Baldwin uses the name Deschutes Formation until a definite correlation with the Dalles Formation can be made and this author will follow suit.

Recently published geologic maps of the Powell Buttes area include a U. S. Geologic Survey Reconnaissance Map of the East Half of the Bend Quadrangle by Swanson (1969), the U. S. Geologic Survey Geologic Map of Oregon East of the 121st Meridian by Walker (1977), and the U. S. Geologic Survey Map of Oregon West of the 121st Meridian by Wells and Peck (1961). Gravity and magnetic anomaly maps by Couch (1978), Pitts and Couch (1978), and Pitts (1979) also are available.

PETROGRAPHY

Introduction

The lavas of Powell Buttes cover approximately 80 percent of the thesis area, with the remainder covered by silt, alluvial fan debris, and aeolian and volcanic sediments. Many of the flows appear very similar to one another in hand specimen, are altered, and are not traceable over large distances; consequently no attempt has been made to map them individually. Instead, the distribution of each distinctive lithology has been mapped as a single homogeneous unit. These distinctive lithologies include rhyolite, rhyodacite, dacite, basaltic andesite, tuffaceous and epiclastic sediments, ash-flow tuffs, and a volcanic conglomerate. (See Plate I)

Petrographic analyses of approximately 55 thin-sections indicate that the rhyolites and dacites are sparsely porphyritic with subhedral to anhedral phenocrysts of quartz in additiona to alkali and/or plagioclase feldspar. Both of these lithologies exhibit extensive devitrification of the glassy groundmass. Alternatively, the basaltic andesite is typically dark and sparsely porphyritic with a pilotaxitic groundmass. Deposits that are of lesser extent include ash-flow tuffs that are moderately to well indurated and composed principally of angular glass shards in addition to pumice, scoria, and lithic fragments.

RHYOLITES

General Statement

The rhyolite flows of Powell Buttes dominate the northern half of the thesis area and occur to a lesser extent in the southern part. The thickness of the rhyolites is extimated to range from 60 to at least 400 m. In outcrop, the weathered surfaces display a range of colors including dark-gray (N3), grayish-red (10 R 4/2), and light-brown (5 YR 5/6). Colors of fresh surfaces include medium dark-gray (N4), grayish red-purple (5 RP 4/2), and dark greenish-gray (5 GY 4/1).

In the field, the rhyolites were observed to have a platy jointing with the joints spaced at intervals from 0.5 to 7.0 cm. Contorted flow-bands from the viscous flow of the rhyolite are often paralleled by the platy jointing (Figure 3). All of the rhyolites are sparsely porphyritic and estimated to contain no more than 15 percent phenocrysts. The phenocrysts evident by examination with a hand lens include subhedral to anhedral quartz and alkali feldspar varying in length from 0.5 to 4.0 mm. Flowbanding is a common texture of the groundmass and is revealed by different colors. Often, the feldspar weathers out leaving small voids in the surface. Locally, the weathered feldspar still remains as kaolinite, with a dull-white, earthy luster, which is easily picked away with a knife point. The quartz averages 2.0 mm in diameter and is readily recognized by its concoidal fracture and vitreous luster.

Petrography

Petrographic analyses of selected thin-sections also reveals that the rhyolites contain phenocrysts of quartz and sanidine in a formerly

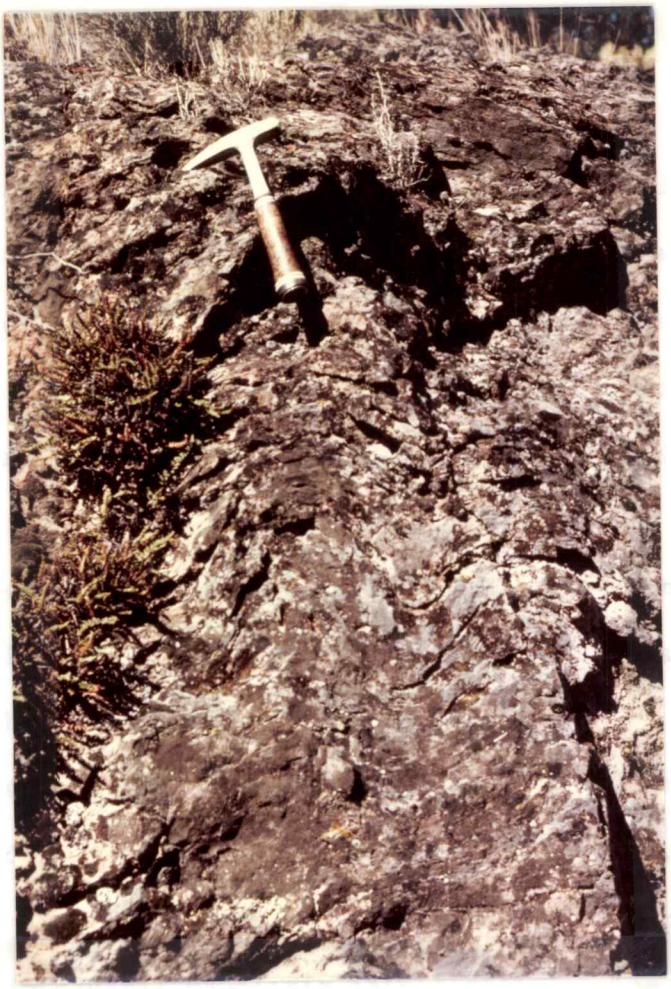

Figure 3. Rhyolite exhibiting platy jointing and folds resulting from flow.

glassy groundmass that typically shows extensive devitrification. The quartz phenocrysts range from 0.2 to 2.0 mm in size and are subhedral to anhedral. Some of the phenocrysts are rounded and show slight embayments from resorption, indicating conditions of changing equilibiria. The quartz also occurs as a product of secondary mineralization, filling veins.

Sanidine phenocrysts range in size from 0.5 to 4.0 mm in length and are subhedral to anhedral with Carlsbad twinning occasionally exhibited. Some of the sanidine phenocrysts show evidence of resorption with slight embayments and rounding. The embayments are filled with groundmass material and in some cases with additional sanidine.

Phenocrysts that are thought to be anorthoclase (Figure 4) have been identified in several rhyolitic thin-sections. The anorthoclase is a high temperature sodium-rich form of sanidine, characteristic of peralkaline rocks (Nockolds, 1978), and exhibits a combination of pericline and albite twinning, giving it a cross-hatched twinning. Optically, the anorthoclase is identified by its low relief, an index of refraction less than balsma, the weak birefringence, and a biaxially negative interference figure with a 2V of 20°.

The rhyolites contain a variety of trace minerals. Zircon occurs throughout most of the thin-sections examined. Typically it is less than 0.1 mm in size and occurs as euhedral, colorless microphenocrysts. It is tetragonal in form with high relief, parallel extinction, and high birefringence. The zircons occur isolated in the groundmass or as glomeroporphyritic clumps (Figure 5). Rarely the zircons may be included in feldspar phenocrysts, indicating the zircons formed early in the melt.

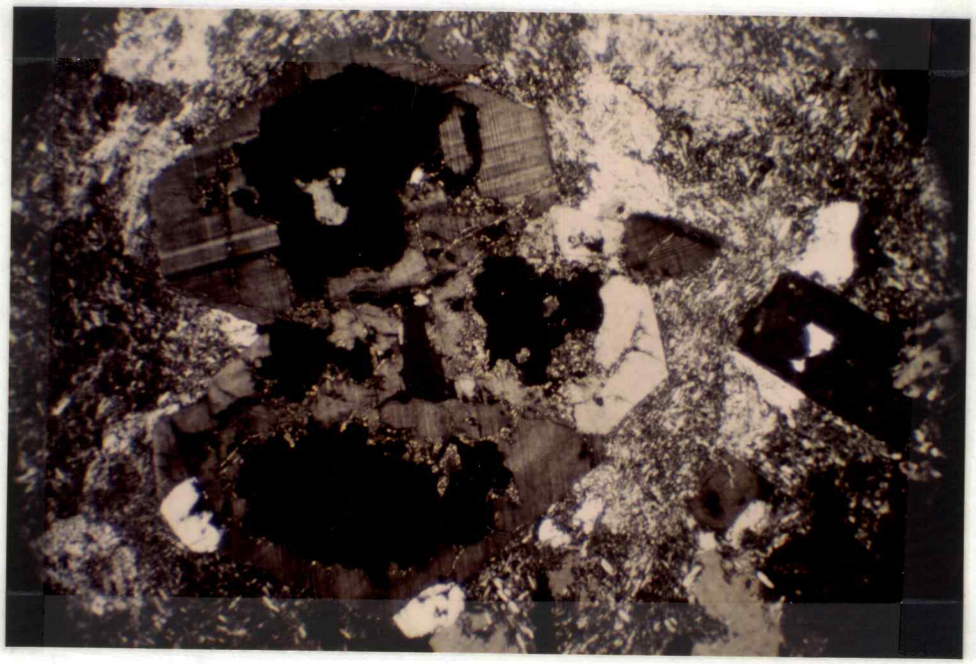

Figure 4. Photomicrograph of anorthoclase with pericline twinning. Cross polarized light. Field of view 4.5 mm.

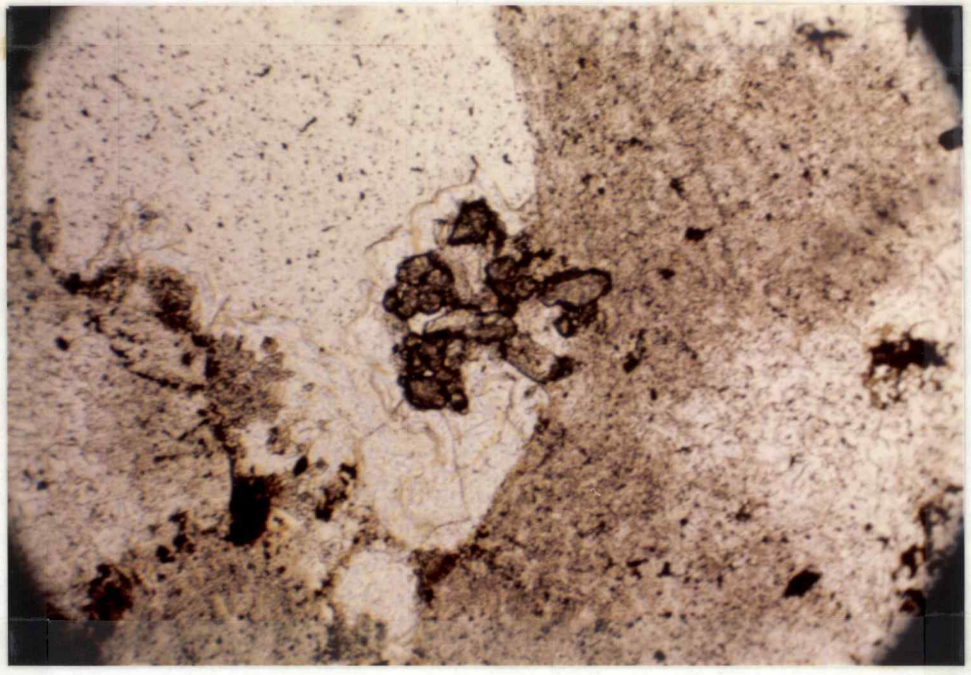

Figure 5. Photomicrograph of glomeroporphyritic zircon. Plane light. Field of view 0.75 mm.

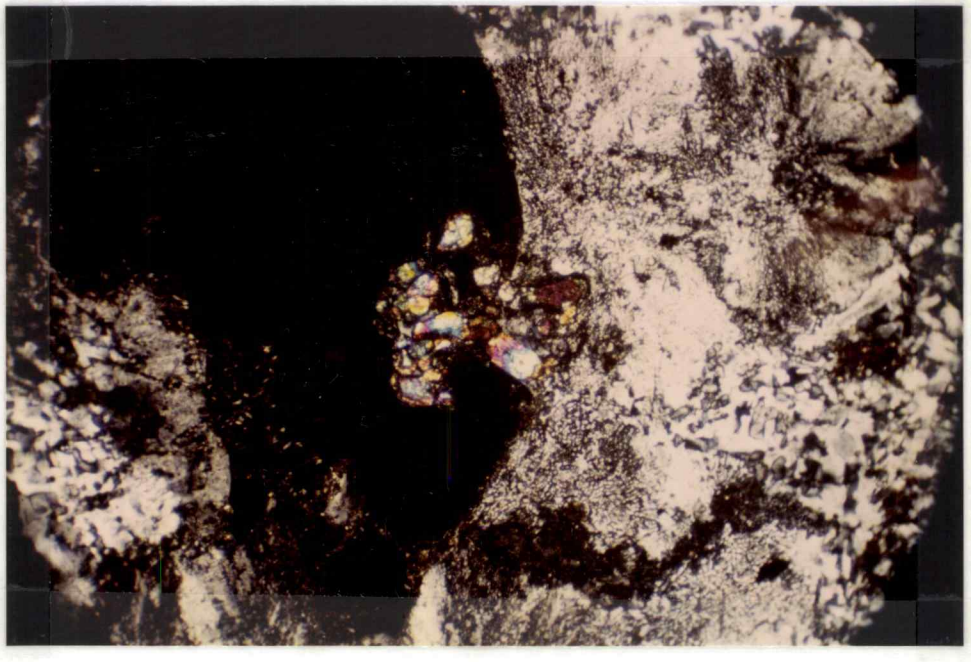

Figure 6. Same as Figure 5, but with cross polarized light.

Some traces of biotite exhibiting resorption were found in the rhyolites of Powell Buttes and average 0.2 mm in length. Deer et al. (1966) note that biotite is expecially characteristic of rocks of calc-alkaline affinity and Larsen et al. (1937) state that when it occurs in extrusive rocks, it may be partially resorbed. Epidote is common in the groundmass of many of the rhyolites studied and averages 0.1 mm in size. No optic sign was obtained because of the small size of the crystals; however, on the basis of the strong birefringence, high relief, parallel extinction, single good cleavage, and greenish-yellow to yellow-green pleochroism, the crystals were tentatively identified as epidote (Figures 7,8) The epidote typically occurs as a deuteric or late stage magmatic mineral and may form from hydrothermal alteration of plagioclase or biotite (Johannsen, 1932; Deer et al., 1966). The crystals commonly appear to have minor alteration on parts of their rims. Kaolinite is also found as a decomposition product of the feldspar and glass in the rhyolites. Brown and green alteration products, probably of the montmorillonite group, were found also in the groundmass. Secondary hematite and to a lesser estent limonite, occur throughout most of the petrographic thin-section, caused by weathering of primary iron minerals such as magnetite.

Traces of an unidentifed alteration of a high relief mineral (Figure 9) are present in the groundmass of several slides. The fragments of this mineral range in size from 0.05 to .4 mm and are strongly pleochroic from a light greenish-blue to a deep grayish-blue with a biaxially negative 2V of 20°. Several of the fragments display the characteristic amphibole cleavage.

Figure 7. Photomicrograph of a spherulitic rhyolite exhibiting orb texture (Lofgren, 1971). Note epidote phenocrysts. Plane polarized light. Field of view 1.5 mm.

Figure 8. Same as Figure 7, but with cross polarized light.

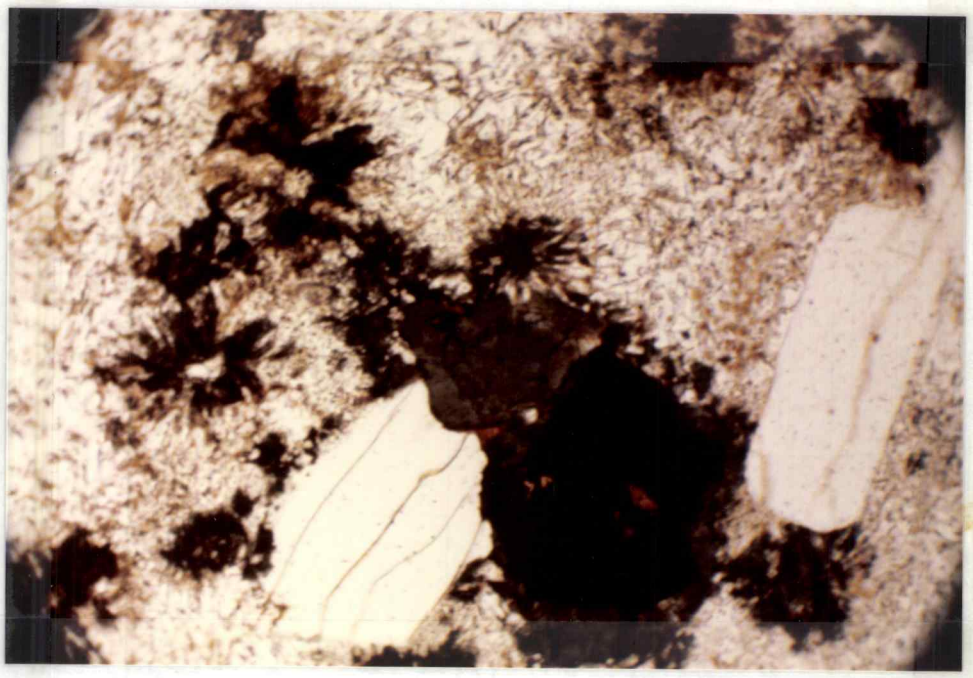

Figure 9. Photomicrograph of amphibole alterd to an unidentified blue-gray mineral. Plane light. Field of view 1.5 mm.

One of the most common alterations shown by the more silicic lithologies of Powell Buttes is devitrification caused by the inherent instability of the original glass. This recrystallization has resulted in the formation of minute grains of feldspar, microspherulites, and a micropoikilitic texture (Jackson, 1970). The micropoikilitic texture (Figure 10) resulted as quartz formed large crystals, poikilitically enclosing the microlites of feldspar. Generally the micropoikilitic quartz crystals appear subspherical and essentially equidimensional, ranging in size from 0.2 to 2.0 mm. Under low magnification the crystal boundaries appear smooth, but higher magnification reveals they are irregular and appear to interdigitate with one another. It was possible to obtain interference figures on some of the subhedral microlites and they were determined to be sanidine. Lofgren (1971) observed that the widespread occurrence of micropoikilitic quartz in rhyolites and its development in experimentally devitrified glasses may be a good indicator of a former glassy state. He also concluded that the micropoikilitic quartz is the result of the initial crystallization of a glass or silicate melt at subsolidus temperatures.

The author has also observed in several rhyolite thin-sections what Lofgren (1971) refers to as an "orb texture". The orb texture consists of a circular volume occupied by a spherulite whose periphery is defined by small (< 0.05 mm) amorphous, spherical bodies called globulites. The orb texture develops as the growing spherulites pushes the globulites ahead of its advancing radial fibers. Spherulites within an orb usually terminate at the edge of the surrounding globulites, but rarely the fibers of the spherulites pass beyond the boundary.

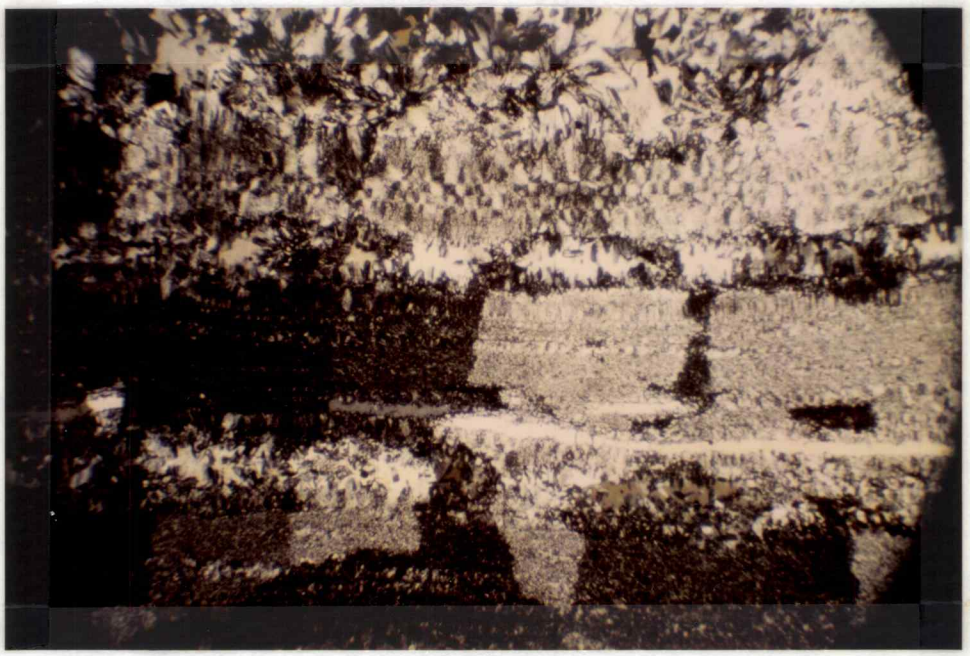

Figure 10. Photomicrograph of devitrified flowbanded rhyolite exhibiting a micropoikilitic texture. Cross polarized light. Field of view 4.5 mm.

According to Lofgren, growth of spherulites is marked by more water or slower cooling rates and consequently higher temperatures for a longer period of time, compared to those of the glassy stage. The higher temperatures are maintained either by slow cooling which permits extensive nucleation and crystal growth, or from reheating with similar results. The higher water content may have accompanied the original magma or have come from outside sources, particularly during reheating, and can be rich in alkalies.

DACITES

General Statement

The dacites of Powell Buttes occur principally in the southwest and central parts of the thesis area. Fresh outcrop surfaces range in color from a medium light-gray (N6) to a grayish-red purple (5 RP 4/2) and grayish-black (N2). Weathered surfaces tend to be medium gray (N5) and some have a mottled appearance. In outcrop, the dacites are often exemplified by a planar jointing ranging from 0.5 to 3.0 cm in width.

Macroscopic examination reveals the dacites to be sparsely porphyritic with subhedral phenocrysts of feldspar, 1.0 mm or less in length, embedded in a dense aphanitic groundmass. Some of the feldspar phenocrysts are now opaque white and easily picked away with a sharp probe, probably having been altered to clay. Commonly the dacites exhibit elongate vesicles 2.0 to 8.0 mm long resulting from flow, whereas other dacites have more rounded to ellipsoidal vesicles ranging from 1.0 to 8.0 mm in diameter. Petrographic examination reveals that some angular voids originally contained plagioclase that has been removed by weathering, as evidenced by remnant plagioclase. Some of the voids also contain secondary anhedral quartz mineralization in addition to quartz filling discontinuous veins.

Petrography

In thin-section, the groundmass of the dacites is typically devitrified glass and contains numerous subhedral microlites of feldspar exhibiting a parallel to subparallel flow alignment around some of the

phenocrysts. The groundmass also in places displays micropoikilitic texture.

Some plagioclase phenocrysts in the dacites are euhedral, but more commonly they are subhedral with the composition of andesine (An_{38} to An_{45}). Embayments of the phenocrysts by the groundmass is sometimes so extensive that only the rim of the phenocryst, which shows Carlsbad or albite twinning, remains. Rarely, pericline twinning is seen. Faint oscillatory zoning (Vance, 1962) is seen in many of the plagioclase phenocrysts (Figure 11).

Patchy zoning is also common in the dacites. Vance (1962) notes that it is especially common in plagioclase-rich volcanic and plutonic rocks of calc-alkaline affinity. This intensive corrosion of the inner, more calcic parts of the crystals, and the subsequent infilling with additional plagioclase, represents a tremendous displacement of equilibria resulting from movement of the magma.

Trace minerals found in the dacites include zircon, magnetite and biotite. The zircons (0.05 mm in size) are subhedral and where found within plagioclase phenocrysts, indicate the early crystallization of the zircon. The traces of biotite are at the most 0.3 mm in length with minor alteration to magnetite. The fragments of biotite have fair relief and are a pleochroic brown or olive-green with the strongest absorption parallel to the lower polarizer. The alteration products of the dacites include hematite and limonite. Kaolinite, and green and brown clays that are probably smectites, are also present.

A glassy dacite is located in the NE¼, SE¼, Sec. 23, T. 16 S., R. 14 E. Fresh surfaces are a grayish-black (N2) and weathered surfaces

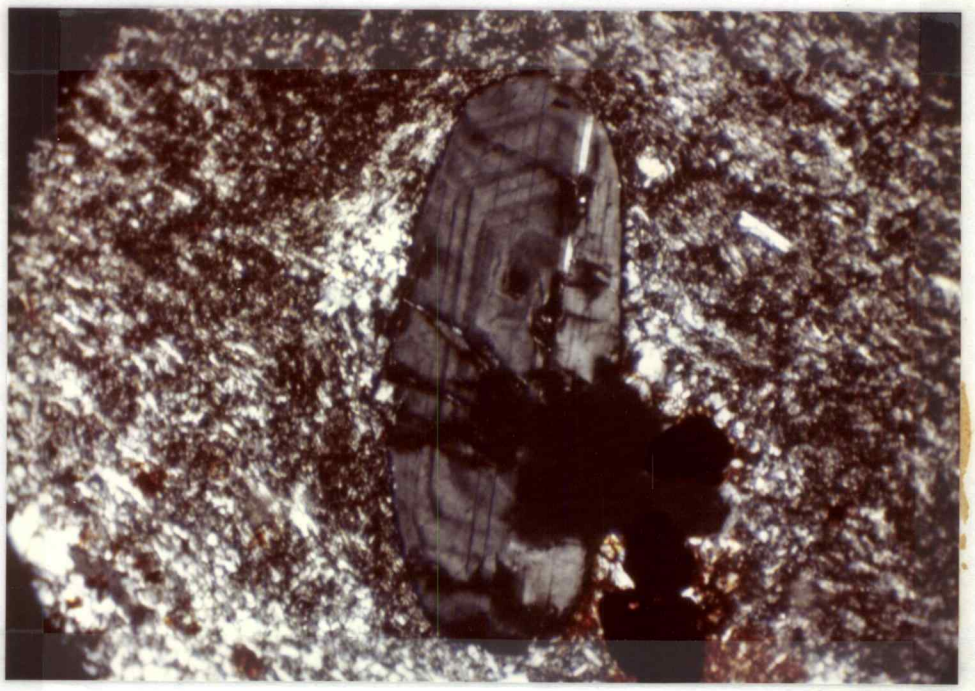

Figure 11. Photomicrograph of a partially resorbed plagioclase phenocryst exhibiting oxcillatory zoning in a dacite. Cross polarized light. Field of view 4.5 mm.

are a dark yellowish-brown (10 YR 4/2). In hand specimen, the dacite has numerous fractures approximately 0.5 mm wide that are stained with limonite.

Petrographic examination reveals the dacite to be porphyritic with a devitrified glassy groundmass. Augite ranges in length from 0.1 mm as granules in the groundmass, to 2.0 mm as anhedral phenocrysts. It is readily recognized by its moderate birefringence, 45° extinction, 2V of 60°, and biaxially positive interference figure. Other features noted in the augite include twinning, the "hourglass" extinction structure, and inclusions of magnetite.

The orthopyroxene hypersthene, also was distinguished in the groundmass by its lower birefringence, parallel extinction, and biaxially negative 2V in excess of 60°. The phenocrysts are typically subhedral laths, approximately 0.3 mm long, with high relief, and a few contain inclusions of magnetite.

The plagioclase phenocrysts all exhibit normal or oscillatory zoning in addition to Carlsbad and albite twinning. The phenocrysts are up to 1.3 mm long and microlites of the groundmass average 0.2 mm. The composition of the phenocrysts is labradorite (An_{52}), while the microlites exhibit normal zoning and have a composition of at least andesine (An_{31}). The author observed several phenocrysts with normal zoning and extensive resorption, giving the phenocryst a "mottled" appearance (Figure 12), yet other phenocrysts in close proximity appear very fresh. The observed phenocmena may have been caused by mixing of magmas or the mottled phenocrysts may have been the primary phenocryst in the melt. If the latter condition prevailed, equilibrium conditions

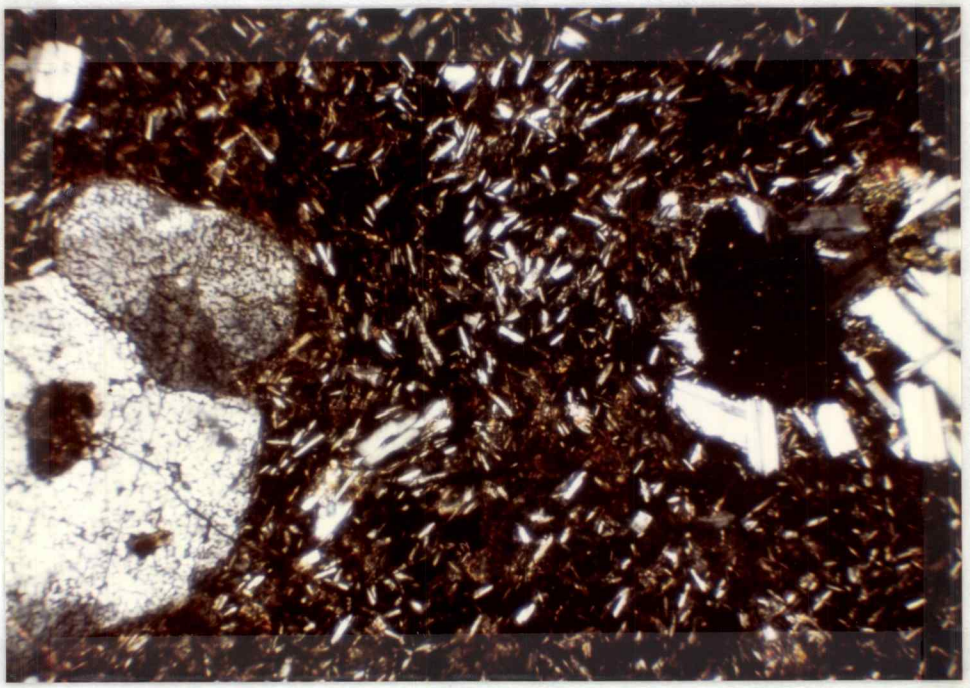

Figure 12. Photomicrograph of plagioclase phenocrysts in dacite exhibiting intense resorption. Note glassy groundmass with plagioclase microlites and minor augite. Cross polarized light. Field of view 4.5 mm.

may have changed slightly, resulting in resorption of the existing phenocrysts and precipitation of fresher, more stable phenocrysts.

The glass of this dacite is almost completely devitrified and magnetite dust is present throughout the slide, with some of the dust altered to limonite. Reflected light also shows kaolinite which displays some limonite staining. The author has also identified a weakly pleochroic substance as smectite (Figure 13), which seems to mantle some of the augite. The smectite is a moderate-to-dark olive-green with high relief and low birefringence. The occurrence of the smectite is probably the product of hydrothermal alteration or weathering of the augite (Deer et al., 1966).

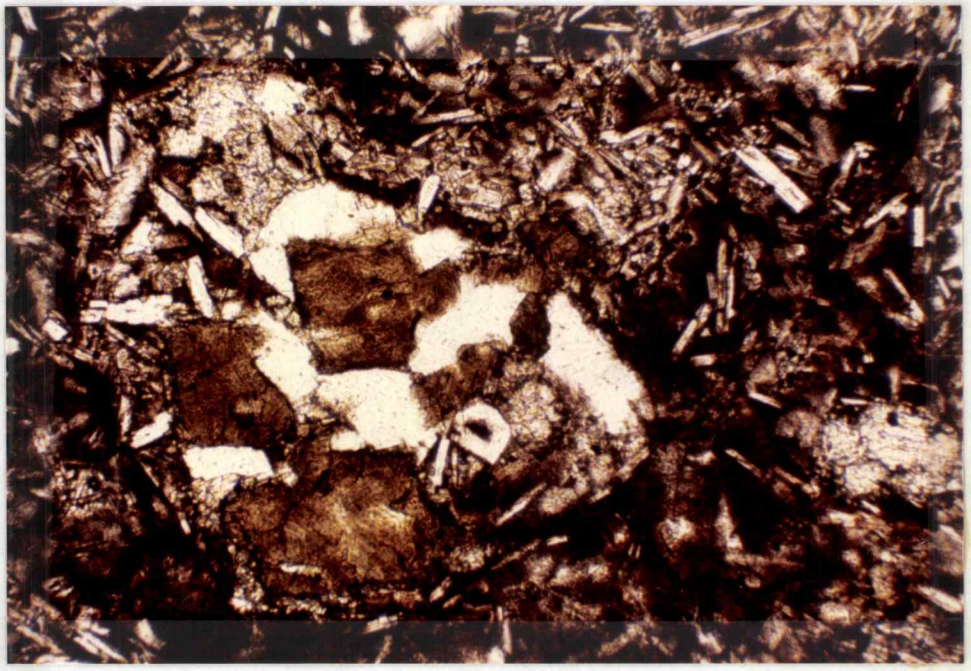

Figure 13. Photomicrograph of augite phenocrysts (left center) mantled with smectite alteration. Plane light. Field of view 4.5 mm.

RHYODACITES

General Statement

Ten rhyodacite of Powell Buttes is located in the NE¼, SE¼, Sec. 13, T. 16 S., R. 14 E. Recognition of this flow is facilitated by its five-sided columnar joints (Figure 14) measuring approximately 12 cm across and the glassy grayish-black (N2) appearance of a fresh surface.

Petrography

Petrographic examination reveals the specimen to be completely devitrified and porphyritic with spherical perlitic cracks (Figure 15) ranging from 1.0 to 4.0 mm in diameter. The phenocrysts within this flow include a clinopyroxene showing evidence of resorption and ranging in diameter from 0.2 to 1.0 mm. Based on the biaxially positive 2V of 60°, the pale greenish color, moderate birefringence, high relief with $n \neq$ balsam, and 40° extinction angle, the clinopyroxene is determined to be augite. Phenocrysts of subhedral to anhedral andesine (An_{35-43}) range in length from 0.3 to 2.0 mm with albite, Carlsbad, and pericline twinning. Some normal zoning is noted in the plagioclase. Inclusions within the plagioclase include fragments of magnetite (0.1 to 0.2 mm) and resorbed augite approximately 0.2 mm in size, indicating early crystallization within the melt. The groundmass consists of microlites of feldspar (Figure 16) less than 0.1 mm in length and exhibiting a sub-parallel flow alignment. Trace amounts of zircon are noted.

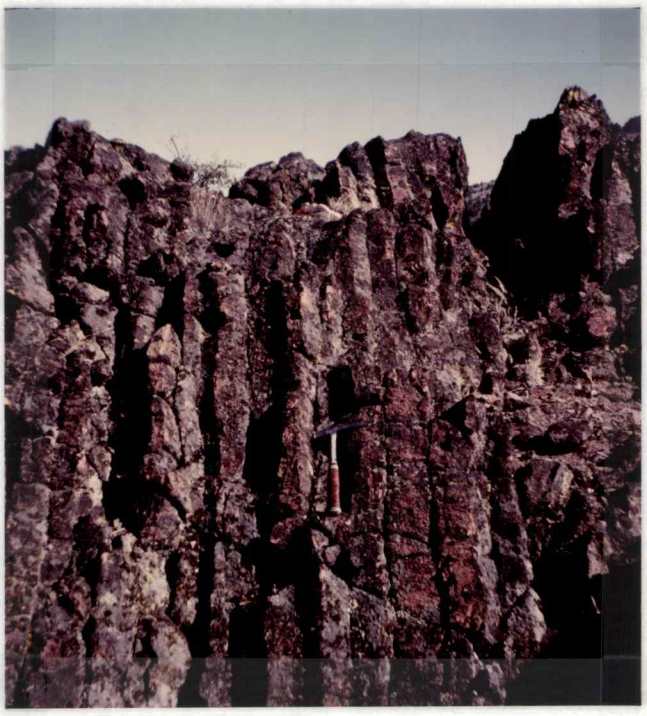

Figure 14. Rhyodacite exhibiting columnar jointing, located in the NE¼, SE¼, Sec. 13, T. 16 S., R. 14 E.

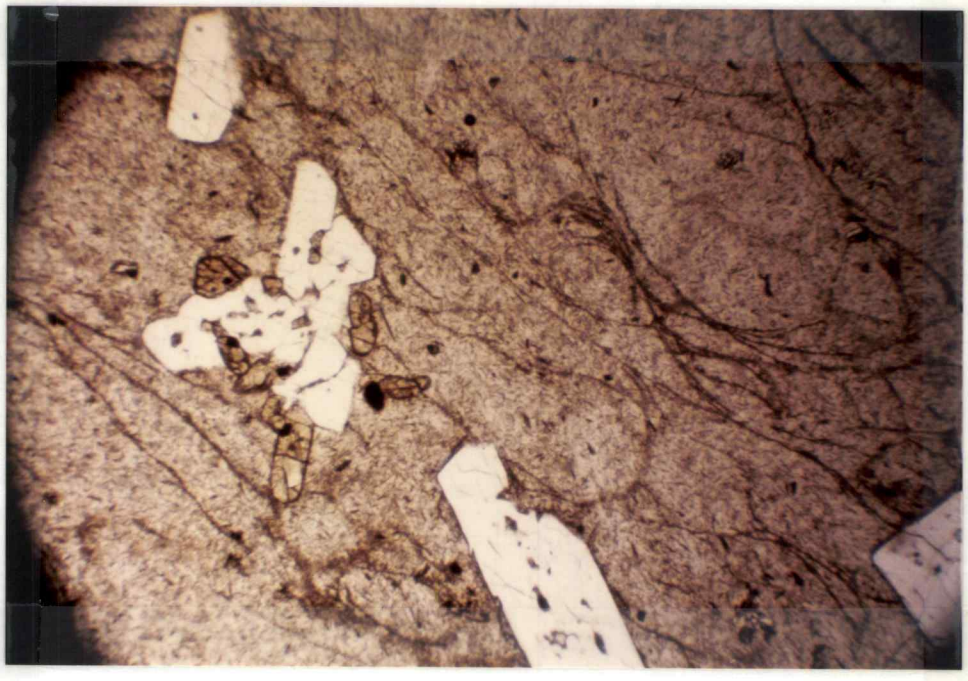

Figure 15. Photomicrograph of columnar rhyodacite with perlitic cracks and glomeroporphyritic clot of plagioclase and augite. Plane light. Field of view 1.5 mm.

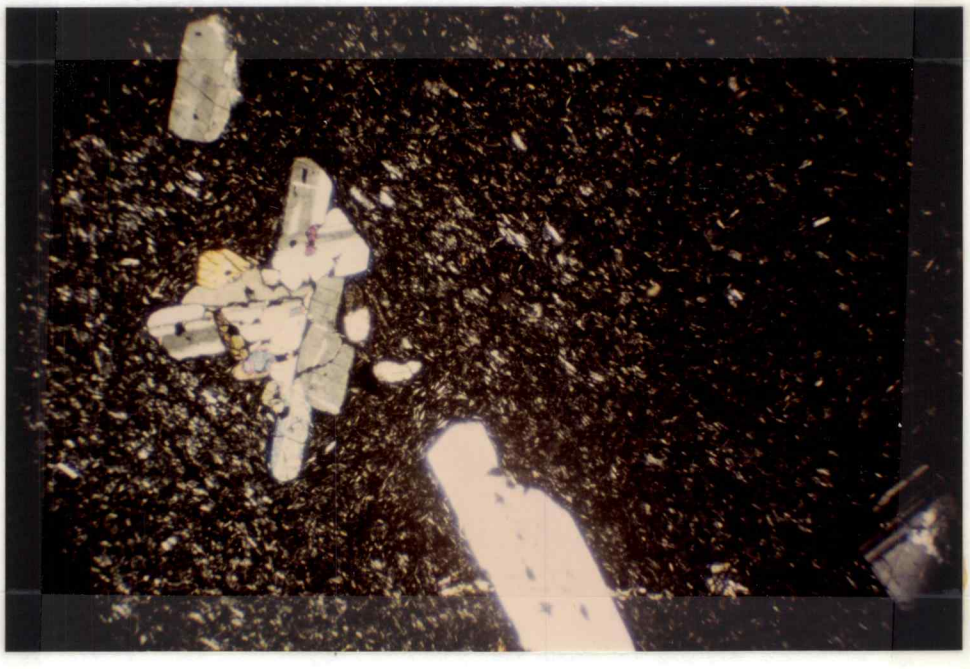

Figure 16. Same as Figure 15, but with cross polarized light.

BASALTIC ANDESITE

General Statement

Several flows of basaltic andesite occur in the southern part of the field area. They are approximately 42 m thick and typically exhibit platy jointing, with the spacing of the joints ranging from 0.5 to 4.0 cm. In outcrop, fresh surfaces of the aphanitic basaltic andesite are a medium-gray (N5) and weathered surfaces are a grayish-red (10 R 4/2) or (5 R 4/2), or a dark-yellowish-brown (10 YR 4/2).

Petrography

The basaltic andesites are sparsely porphyritic with a pilotaxitic groundmass texture. The plagioclase phenocrysts are subhedral, are approximately 1.0 mm in length, and have a composition of An_{67}. Carlsbad and albite twinning are common features of the phenocrysts and minor pericline twinning is also noted. Some resorption of the plagioclase phenocrysts has been observed. The plagioclase microlites of the groundmass are labradorite (An_{52}) and 0.1 mm or less in size.

Augite is also a prominent phenocryst, ranging in size from 0.5 to 1.0 mm, and small granules (0.05 mm) of pyroxene are scattered throughout the groundmass. The "hourglass" extinction structure is commonly noted (Figure 17) and the augite displays optical characteristics similar to the augite in the dacites noted in the previous section.

A trace of biotite is present, along with small granules of magnetite 0.05 mm in diameter. An alteration product, that may be celadonite, is present on some of the plagioclase phenocrysts. The mineral is yellowish-green, finely crystalline, and slightly birefringent

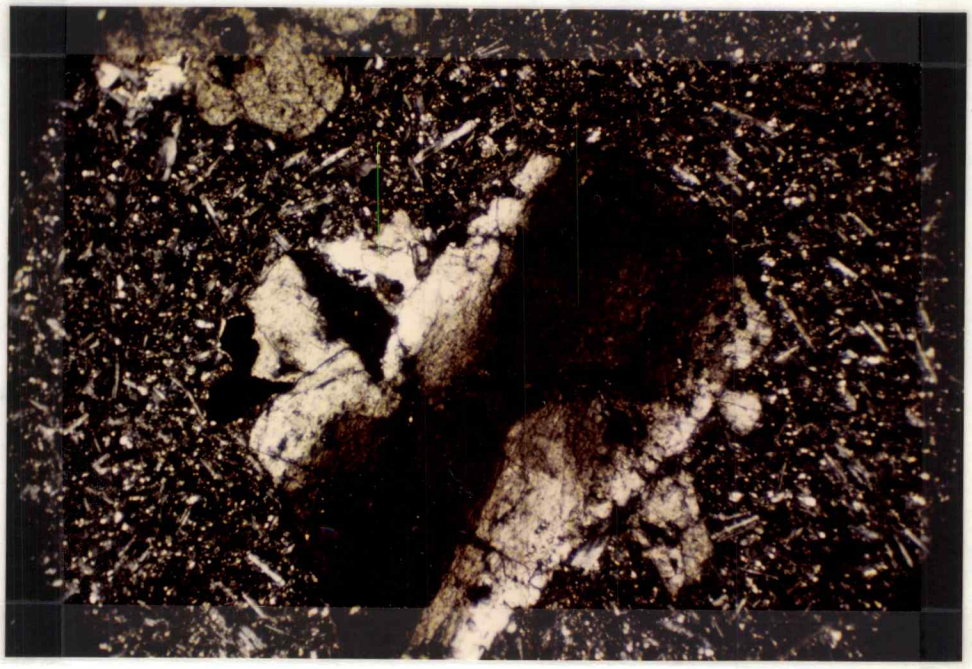

Figure 17. Photomicrograph of basaltic andesite with an augite phenocryst exhibiting the "hourglass" extinction structure in a groundmass with plagioclase microlites, magnetite, and pyroxene granules. Cross polarized light. Field of view 1.5 mm.

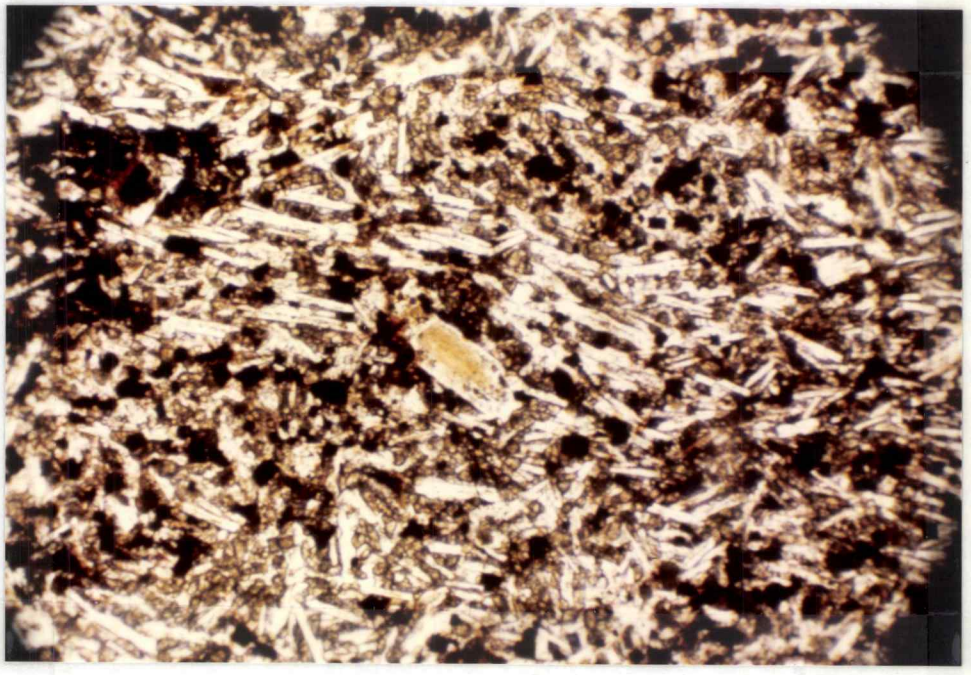

Figure 18. Basaltic andesite with plagioclase phenocryst exhibiting celadonite alteration. The groundmass is composed of plagioclase microlites, pyroxene granules, and magnetite. Plane light. Field of view 1.5 mm.

(Figure 18). No interference figure was obtained. The alteration is restricted to the cores of the phenocrysts and is bounded by a thin rim of plagioclase (An_{35}) that exhibits Carlsbad or albite twinning in some examples. Hematite staining is also present.

ASH FLOWS

General Statement

Most of the vitric ash-flow tuffs of Powell Buttes were not traceable across the field area as marker beds, but instead occur as small isolated outcrops. All of the ignimbrites are moderately to intensely welded and in thin-section usually display extensive devitrification of the glass. The explosive nature of the process by which these deposits were formed is indicated by the angular glass shards, fractured crystals, vitric dust, and angular lithic fragments. Some of the ignimbrites of Powell Buttes exhibit moderate deformation of the virtroclastic textures; some none at all. Several of the petrographic slides contain fragments of pumice 1.0 mm in diameter that have undergone complete collapse of the pore spaces and have been welded into a compact glass. The tubular nature of the pores in the original pumice structure is still evident. Compression and molding of the plastic glass shards against phenocrysts is also noted. Trichites (Johannsen, 1932a) are present in one specimen and traces of epidote are found in a few samples.

Petrography

The most extensive lapilli ash-flow tuff is located south and west of Hat Rock. Excellent exposures of this very pale-green (10 G 8/2) lapilli tuff are found in the NW¼, SW¼, Sec. 18, T. 16 S., R. 15 E. The ash flow is porous, moderately indurated and contains subrounded pumice lapilli up to 4.5 cm in size, with a few smaller lithics of basaltic andesite averaging 3.0 mm in length (Figure 19).

Figure 19. Lapilli ash-flow tuff located south of Hat Rock.

The groundmass was originally composed of many angular glass shards and bubble walls approximately 0.5 mm in size. Meteoric water circulating through the porous system has been responsible for the hydration and solution of the glass shards. The resulting cavities are now rimmed or completely filled with a pseudomorphous precipitate of an authigenic zeolite forming an axiolitic texture (Figure 20). The zeolite was identified as clinoptilolite by X-ray diffraction of a bulk sample. Optically, the zeolite is finely fibrous and exhibits moderate relief with an index of refraction less than balsam. Minor celadonite has also filled some of the cavities that are not completely filled with zeolite. The celadonite is light-green, and exhibits fair relief. A devitrified groundmass surrounds the glass shards. X-ray diffraction was used to identify high sanidine and tridymite in the specimen.

Petrographic examination also revealed the inclusion of a devitrified lithic fragment, 1.0 cm long, of an older welded tuff. This fragment shows more extensive compression of the glass shards, and the pore spaces of pumice within the fragment have been filled with quartz during vapor-phase alteration. Also noted in the groundmass were a few traces of andesine (An_{48}) phenocrysts exhibiting oscillatory zoning and Carlsbad or albite twinning. Celadonite and probable smectites are responsible for the characteristic green color of this tuff. Minor kaolinite and hematite also were noted.

An excellent example of a welded tuff showing no compaction is located in the SE¼, NE¼, Sec. 13, T. 16 S., R. 14 E. The tuff lacks compaction because insufficient heat was retained to create extensive adhesion of the glass shards and subsequent merging with one another.

Figure 20. Ash-flow tuff with authigenic clinoptilolite in glass shard cavities. Note minor celadonite in center of former shard. Plane light. Field of view 2.5 mm.

A lack of overlying material may have also been a contributing factor. In hand specimen, the tuff is a light pinkish-gray (5 YR 6/1) and exhibits abundant angular glass shards ranging in length from less than 1.0 mm to 5.0 mm. The specimen has undergone extensive devitrification and many of the glass shards are rimmed with devitrified glass displaying a "salt and pepper" appearance (Figure 21). The center of some of these shards is fibrous, and probably consists of alkali feldspar and cristobalite. Anhedral quartz crystals approximately 0.3 mm in size were observed to interpenetrate in the groundmass.

Another rhyolitic vitroclastic tuff in the NE¼, NW¼, Sec. 3, T. 16 S., R. 15 E., exhibits glass shards with a well developed axiolitic texture (Figure 22). According to Nockolds (1978) this texture forms in Tertiary or younger ash flows from the replacement of the glass shards with a very fine-grained parallel intergrowth of feldspar and cristobalite. The two minerals began their crystallization at the margin of the shard and moved inward to meet at a central discontinuity, marked by a dark line. This tuff also contains phenocrysts of sanidine up to 2.0 mm long with fine trains of magnetite dust incorporated in the crystals near the rim during crystallization. Subhedral and anhedral quartz phenocrysts, up to 3.0 mm long, also are present. The phenocrysts make up to 15 percent of the specimen.

A pale red-purple (5 RP 6/2) vitroclastic breccia is located in the NW¼, SE¼, Sec. 18, T. 16 S., R. 15 E. The specimen is porous and contains many subangular fragments of an earlier, but similar, vitric tuff which range in length from 0.1 to 6.0 cm. These fragments are

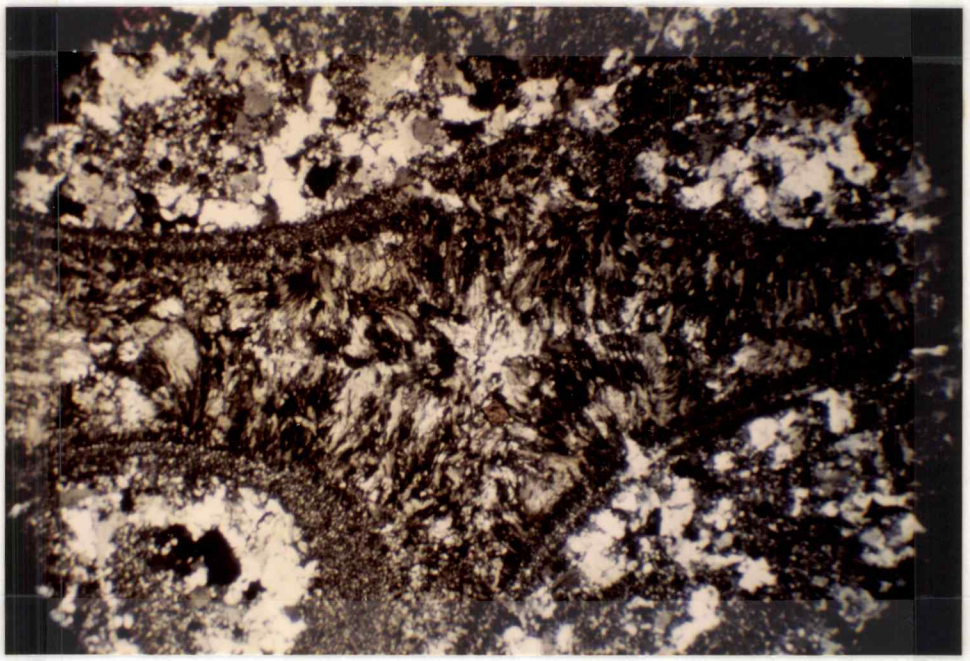

Figure 21. Photomicrograph of devitrified glass shard from tuff located in the SE¼, NE¼, Sec. 13, T. 16 S., R. 14 E. Cross polarized light. Field of view 4.5 mm.

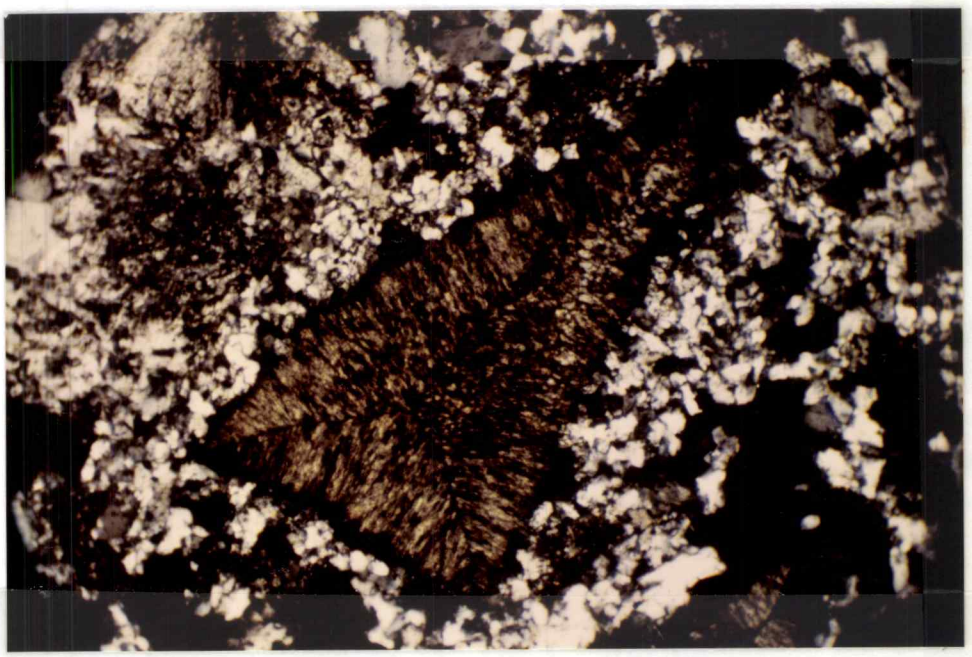

Figure 22. Photomicrograph of devitrified glass shard located in the NE¼, NW¼, Sec. 3, T. 16 S., R. 15 E., exhibiting the axiolitic texture. Cross polarized light. Field of view 2.5 mm.

easily discerned in hand specimen because they are not as completely oxidized as the groundmass. Other fragments that are less numerous include angular lithic fragments of basaltic andesite ranging in length from 0.1 to 2.0 cm, and minor scoria 0.2 to 1.0 cm in diameter. Sub-rounded and partly collapsed pumice lumps 0.1 to 1.0 cm in diameter also are present. Petrographic examination reveals that the tuff has been devitrified and is only siightly birefringent. The vitroclastic groundmass and brecciated tuff fragments exhibit similarities in the size of the crystallites (0.1 to 0.05 mm), degree of incipient welding, and the even distribution of magnetite dust. These characteristics suggest two similar closely spaced eruptions. Some of the brecciated fragments exhibit serrated edges and the varying extent of oxidation helps to distinguish the groundmass from the brecciated fragments. A few traces of oligoclase (An_{28}) phenocrysts, less than 1.0 mm in length were observed. Hematite staining was also noted with reflected light. X-ray diffraction was used to identify high sanidine and tridymite in a bulk sample.

The SE¼, Sec. 13, T. 16 S., R. 14 E. contains several exposures of a distinctive vitroclastic breccia with angular fragments of rhyolite. The rhyolite fragments are a grayish-red (5 R 4/2), angular, and up to 4.0 cm long. The matrix is aphanitic and a very pale-orange (10 YR 8/2). Petrographic examination shows that the matrix consists of angular glass shards (averaging 0.5 mm long) that have completely devitrified. The rhyolite fragments have also devitrified and contain microspherulites, 1.0 mm in diameter, which exhibit orb texture. The spherulites are also stained with hematite and some glomeroporphyritic zircon has been observed in the rhyolite. Microlites of

sanidine in quartz are also evident in the rhyolite. Kaolinite alteration and some limonite staining are evident in the matrix.

The author has also observed an ash-flow, located in the SW¼, NE¼, Sec. 26, T. 16 S., R. 14 E., with a completely devitrified glassy matrix xomposed of crystalline microlites of feldspar. The only evidences indicating the ash-flow origin of the deposit are several isotropic patches of glass up to 4.0 mm long. The glass resembles collapsed pumice lumps in shape, but occurs in varying orientations throughout the slide. This suggests the possibility of flow as a rheoignimbrite. Also observed were several isotropic angular patches (0.75 mm long) that resemble former glass shards. Remnants of subhedral phenocrysts of sanidine and oligoclase (An_{24}) rim voids in the specimen. Anhedral quartz phenocrysts 0.2 to 0.5 mm have also resulted from devitrification of the glass. Magnetite dust is present throughout the specimen and hematite alteration is noted.

The type of eruption that is probably responsible for these deposits is the Pelean. The initial stages of activity from such an eruption are characterized by nuees ardentes. Short thick flows and/or domes of viscous magma also are common, but are not necessarily associated with the eruptive activity. McBirney (1979) observes that steep-sided domical masses of viscous lava are usually preceded by discharges of a more fluid, gas-rich magma, but that domes do occur without these precursory explosions and the explosions may continue during the rise of the dome. The author has noted that some of the welded tuffs and lapilli tuffs are especially common around the silicic domes of Powell Buttes.

Explosions preceding the activity of the domes may be relatively mild and hurl out angular lithic fragments along with ash and pumice. Alternatively, more powerful explosions may give rise to nuees ardentes. If the nuees ardentes occur during the initial stages of the domes they will consist almost completely of a fresh effervescing magma, expanded to an essentially fluidized condition, which will flow very rapidly over great distances. However, if the nuees ardentes occur after the dome has grown to considerable size, the gas-charged magma will contain quantities of solid blocky debris. Smith (1960) and Ross and Smith (1960) have also observed that deposits formed from domes are usually of restricted volume and distribution.

Hay (1963, 1978) describes the occurrence of a clinoptilolite facies in the John Day Formation near Mitchell, Oregon. From his observations, Hay has concluded that the glass shards have been replaced with clinoptilolite by solution. Walker (1970) has also observed that the diagenesis of the vitric material in Miocene and older ash-flow tuffs in Oregon has resulted in the formation of zeolites, principally clinoptilolite. Barrows, (1960) notes that porposity and permeability are among the major factors controlling the degree of alteration. Poorly welded tuffs and loosely consolidated tuffaceous sediments provide an excellent environment for replacement reactions. Densely welded tuffs are not receptive to such hydrologic processes, except where circulating solutions have gained access through fractures or perlitic cracks.

VOLCANIC DOMES

Eleven volcanic domes ranging in area from 0.05 to 1.95 km^2 are evident at Powell Buttes. There are several rhyolite domes located in the SE¼, Sec. 23, T. 16 S., R. 14 E. which form a nested set. Another group of five small near-surface rhyolite domes trend northeast-southwest on the southeast edge of Powell Buttes. Two other major domes are located on the western half of the Buttes. The largest is an exogenous dome (Figure 23) composed of flowbanded rhyolite. It covers parts of Sec. 10, 11, 14, and 15 of T. 16 S., R. 14 E. In outcrop, the rhyolite of the dome is a grayish yellow-green (5 GY 7/2) with well developed flowbands (Figure 24). The characteristic green-to-greenish white color is probably caused by the development of smectites and kaolinite, mainly from deuteric alteration and, to a lesser extent, from weathering processes. Platy jointing is common with joint spacings ranging from 0.5 to 6.0 cm. The viscous nature of the flow is evident from convoluted banding that can be seen locally in outcrops. Petrographic examination of the rhyolite shows extensive devitrification of the original glass with many fibrous aggregates of alkali feldspar averaging 0.2 mm inlength. In some cases the alkali feldspar forms spherulites 0.4 mm indiameter. Discontinuous veins of secondary anhedral quartz, averaging 1.0 mm in width, parallel the flow-bands. Also observed were subhedral microlites of sanidine, approx-imately 0.1 mm long, with minor zircon and to a lesser extent, biotite.

The other prominent dome (Figure 25) lies in the SE¼, Sec. 14, T. 16 S., R. 14 E. and the circular nature resembles a plug that was

Figure 23. Rhyolite exogenous dome covering portions of Sec. 10, 11, 14, and 15 of T. 16 S., R. 14 E.

Figure 24. Flowbanded rhyolite with platy jointing from the dome in Figure 23.

Figure 25. Rhyolite dome located in the SE¼, Sec. 14, T. 16 S., R. 14 E.

formed when the extruded lava congealed in an area probably not much wider than its feeding conduit. The rhyolite composing this dome is a dark greenish-gray (5 YR 4/1) porphyritic rhyolite with phenocrysts of subhedral quartz up to 3.0 mm in size, and subhedral sanidine up to 4.0 mm in length. The groundmass is aphanitic and exhibits flow around many of the phenocrysts. Petrographic examination reveals extensive devitrification of the glassy groundmass. Fibrous alkali feldspar spherulites predominate in the groundmass and magnetite dust is scattered throughout. Quartz and sanidine phenocrysts both exhibit slight embayments filled by the groundmass and some of the sanidine displays Carlsbad twinns. The flowbanding (Figures 26, 27) is especially evident in thin-section and kaolinitic alteration is also noted.

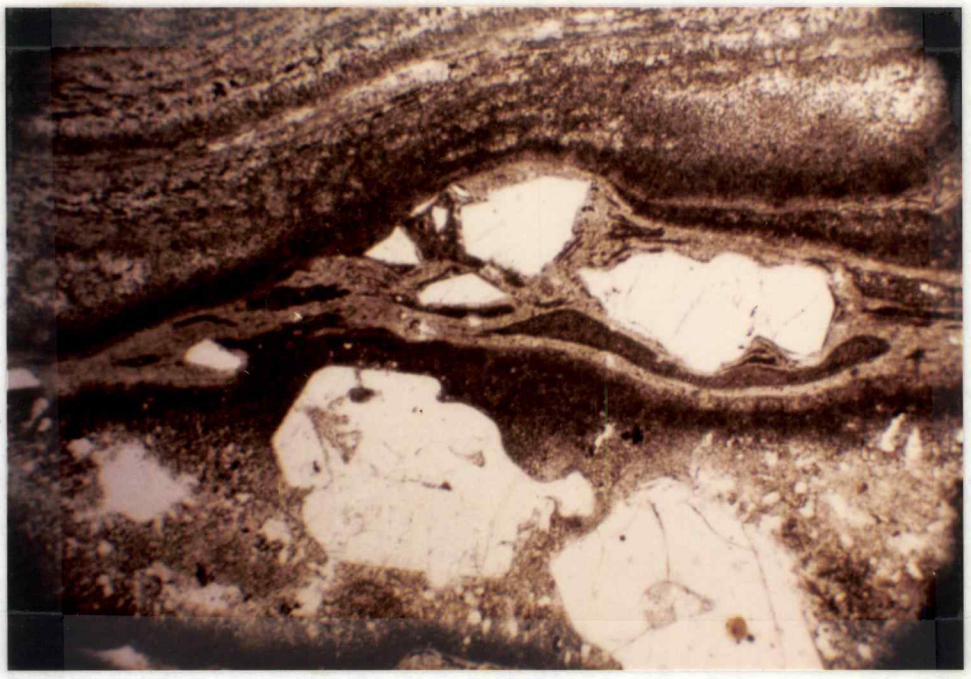

Figure 26. Flowbanding in rhyolite from dome in Figure 25. Plane light. Field of view 4.5 mm.

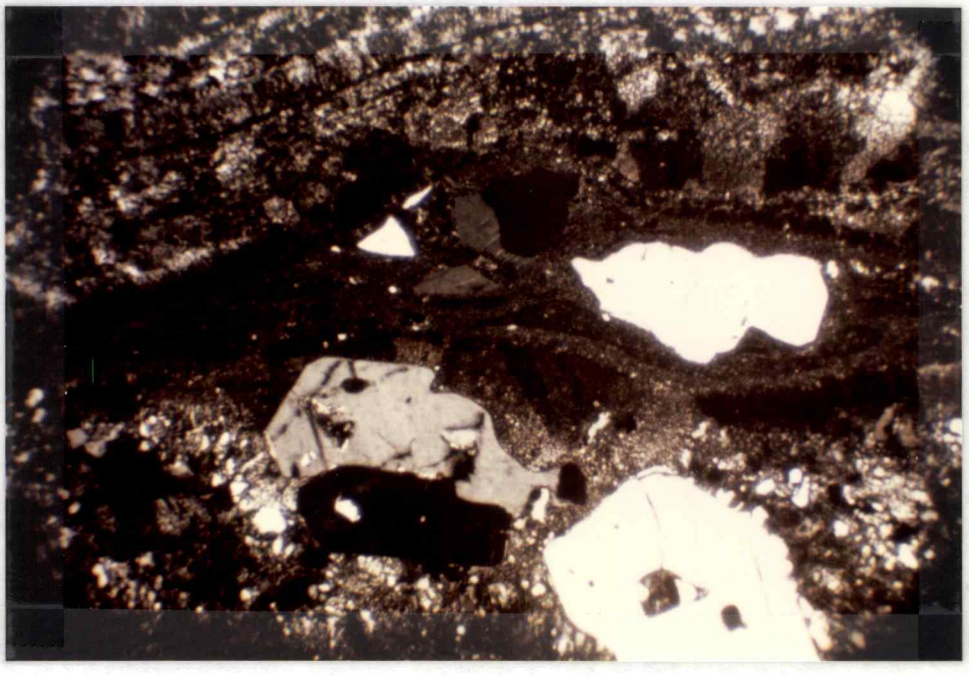

Figure 27. Same as Figure 26, but with cross polarized light. Note devitrified glassy groundmass, embayed sanidine phenocryst (left center), and quartz phenocryst (lower right corner). Field of view 4.5 mm.

SEDIMENTS

Unconsolidated, fine-grained tuffaceous sediments occur in the SE¼, Sec. 11, T. 16 S., R. 14 E. These sediments range in color from a dark yellowish-orange (10 YR 6/6) to a very light-gray (N8) or a pinkish-gray (5 YR 8/1); they are of airfall origin, related to the vent activity of Powell Buttes. This is demonstrated by the fine-grained, uniform nature of the sediments. Weathering has obscured any original bedding in the sediments. Other exposures of air-fall tuffs are located around the rhyolitic dome in the SE¼, Sec. 14, T. 16 S., R. 14 E.

Some of the tuffaceous sediments have been consolidated into siltstones and claystones that lack internal current structures. Very fine-grained tuffaceous sediments that are a grayish-orange (10 YR 7/4) to a dark yellowish-orange (10 YR 6/6) are also evident in the NE¼, SW¼, Sec. 29, T. 15 S., R. 15 E. The tuff contains unidentifiable carbonized plant remains, with several paleosoil horizons, and is unconformably overlain by a thin remnant of a rhyolite flow (Figures 28, 29).

A volcanic conglomerate, consisting mainly of subangular rhyolite boulders and cobbles, with some pebbles, is well exposed in the SE¼, SW¼, Sec. 9, T. 16 S., R. 15 E. (Figures 30, 31). The lithic fragments are contained in a clay matrix with calcium carbonate cement. The author has also observed some minor spring activity in this conglomerate of probable mudflow origin.

Figure 28. Outcrop of tuff with carbonized plant remains located in the NE¼, SW¼, Sec. 29. T. 15 S., R. 15 E. Note rhyolite flow unconformably overlying tuff.

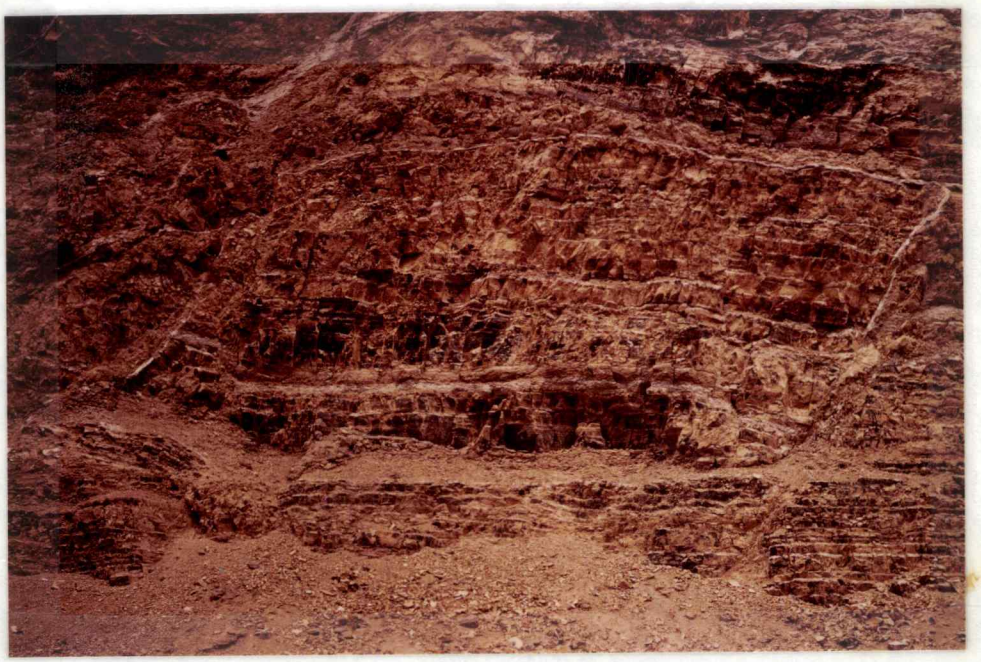

Figure 29. Close up of tuff in Figure 28. Note carbonized plant remains and paleosoil horizon approximately one third of the way up from the base of the photo. Caliche forms white vein fillings.

Figure 30. Volcanic conglomerate located in the SE¼, Sec. 9, T. 16 S., R. 15 E.

Figure 31. Close up of volcanic conglomerate shown in Figure 30.

QUATERNARY DEPOSITS

Quaternary alluvium fills most of the canyons and valleys to an estimated depth of several meters. The material originated from the surrounding slopes and is loosely consolidated. Intermittent streams have conveyed much of this material out of the canyons to form broad alluvial fans on the surrounding plain.

Slumping has occurred in several areas. The dacite ridge southwest of Hat Rock (Figure 32), in the NE¼, SW¼, Sec. 13, T. 16 S., R. 14 E., overlies a lapilli-tuff, probably altered to smectites. The tuff is unstable when wet and has allowed blocks of the overlying dacite ridge to slump slightly, creating prominent slickensides on some of the blocks. Further slumping is evident in the SE¼, SW¼, Sec. 8, T. 16 S., R. 15 E. At this locality the dacite and overlying regolith have slumped leaving a prominent curved surface of rupture or pullaway scarp.

Talus deposits commonly lie on or at the base of the steeper slopes. The talus is typically rhyolite and ranges in size from cobbles to large boulders several meters in size.

A fine white (N9) airfall pumice (Figure 33) is exposed in several areas, and is exposed best in SE¼, SW¼, Sec. 10, T. 16 S., R. 15 E. and the NE¼, NE¼, Sec. 36, T. 15 S., R. 14 E. The pumice ranges in size from 0.25 to 2.0 mm and probably represents the distal part of the Pleistocene Bend Pumice (Taylor, 1980a,b). Overlying the Bend Pumice is a fine soil of aeolian origin.

Figure 32. Erosional remnant Hat Rock (left center). Dacite ridge (right center) has slickensides on some of the blocks from slumping.

Figure 33. Airfall Bend Pumice located in the SE¼, SW¼, Sec. 10, T. 16 S., R. 14 E.

STRUCTURE

The structural relations of Powell Buttes are well defined in the southern half of the thesis area. The dacite, basaltic andesite and rhyolite have been moderately tilted to the southeast with an average dip of 24°. The Reconnaissance Geologic Map of the East Half of the Bend Quadrangle (Swanson, 1969) infers a northeast-southwest syncline located approximately along the southeast edge of Powell Buttes. The structural interpretation by Swanson (1969) suggests that the tilted strata represents the northern limb of the syncline. The structure of the northern half of the thesis area is not easily discerned because of the poor exposure and the banding within the rhyolite flows. The northern front of the Buttes exhibits a terraced appearance suggesting several superimposed rhyolite flows.

Five small (0.05 km^2) near-surface extrusions of rhyolite also are located on the southeast edge of Powell Buttes. The domes form a distinctive lineation implying the presence of an underlying structural weakness or pre-existing fracture which served to channel ascending magmas.

The author suggests that an east-west-trending normal fault 7.4 km long traverses the central area of Powell Buttes. The fault is defined by a subtle lineation on aerial photographs. Field evidence shows an abrupt lithologic change from dacite to rhyolite across the fault. The author has estimated at least 300 m of displacement by comparingthe highest exposure of dacite with the lowest exposure of rhyolite on opposite sides of the fault.

Pitts (1979) notes that there is a high positive gravity anomaly associated with Powell Buttes and a close correlation of positive residual gravity anomalies withknown vent complexes. The vent complexes range in composition from andesite to rhyolite and from Oligocene to Holocene in age. It is the conclusion of Pitts that an olivine-gabbro residuum, resulting from a differentiation process that yielded large volumes of silicic extrusives, is responsible for the closed positive anomalies. Pitts employed simple horizontal cylinder models and three-dimensional bodies of elliptical cross section to determine that the bodies responsible for the positive residual anomalies range in depths from 4.5 to 9.0 km.

The differentiation of large volumes of silicic extrusives, as suggested by Pitts, would require a tremendous amount of mafic and intermediate magma and therefore these magmas should be even more abundant than the silicic lavas. Another problem associated with his hypothesis is that the mafic and intermediate residual rocks are not exposed in old, deeply-eroded calc-alkaline belts. Thus, other possibilities, such as a silicic body at depth, should be considered.

ECONOMIC GEOLOGY

Geothermal Activity

The author has verified two reported occurrences of warm wells on the northern side of Powell Buttes. One well, with an approximate temperature of 32°C, is located in the NE¼, NE¼, Sec. 36, T. 15 S., R. 14 E. and the other is located in the NE¼, NE¼, Sec. 29, T. 15 S., R. 15 E. and has a temperature of 14°C at 82 m. Other warm wells have been reported, but remain unverified by the author. The temperature irregularities at Powell Buttes may arise from differences in the permeability of the rock and/or varying influxes of colder water.

The geothermal activity at Powell Buttes is anomalous for an old silicic volcanic center of John Day age. MacLeod et al. (1977) have observed that most potential geothermal areas are in or near areas of young silicic volcanic fields with cooling intrusive bodies as their heat source. Rhyolitic bodies are the most favorable magmatic heat reservoir because of their generally large size and equant shape in the shallow curst. Lachenbruch et al. (1976b) concluded from their study of the Long Valley Caldera of eastern California that any large rhyolitic body older than 2 m.y. would have cooled to near ambient temperatures. In order for such a body to remain molten it would be necessary to resupply it with heat from deep crustal or subcrustal magmatic sources (Lachenbruch et al., 1976a). Another active geothermal area with characteristics similar to Powell Buttes is the Salton Sea in California (McNitt, 1963), which has both positive gravity and magnetic anomalies. The anomalies at the Salton Sea coincide

with both a thermal anomaly and rhyolitic domes, indicating a cooling intrusive body at depth from which the domes were extruded. Positive gravity and magnetic anomalies are also noted at Casa Diablo, California (McNitt, 1963). The Geysers, California has a pronounced 25 mgal gravity low (Goff et al., 1977) suggesting a molten silicic magma at a depth of 10 km (Isherwood, 1976).

The previously mentioned studies imply an association of positive gravity anomalies with geothermal activity. This may indicate a relation exists between the positive gravity anomaly of Powell Buttes and geothermal activity. Other factors that may be present to resupply the heat necessary to maintain temperatures sufficient for geothermal processes include: 1) hydrothermal circulation in progressively deepening fractures, 2) the upper crustal intrusion of magmatic bodies, and 3) convection from an existing magma chamber extending down through the lower crust.

Uranium Mineralization

Uranium mineralization thought to be meta-autunite (Matthews, 1956), has been associated with mercury in Sec. 13, T. 16 S., R. 14 E. (Peterson, 1958). Exploraton has been by hand mining methods and failed to uncover any significant quantities of U_3O_8 mineralization. The anomalous radioactivity (Matthews, 1955; Schafer, 1956; and Peterson, 1958) occurs in the rhyolites as iron-oxide/hydroxide coatings of fractures and joints in small isolated occurrences. The radioactivity also has been associated with a hyaline opal that fluoresces greenish-yellow. It is suggested by Schafer (1956), that

the U_3O_8 mineralization was concentrated by descending ground water through fractures or ascending vapors derived from cooling magma and transported through the joints and fractures.

GEOCHEMISTRY

Chemical analyses of representative lithologies from Powell Buttes indicate that basaltic andesite, dacite, rhyodacite, and rhyolite are present. The chemical analyses and sample locations are shown in Appendix A; Harker diagrams illustrating the plots of the major element oxides are contained in Appendix B. The author has supplemented the chemical analyses of Powell Butte rocks with those of the John Day Formation from Hay (1963a,b), Peck (1964), Fisher (1966), Robinson (1969), and Oles and Enlows (1971). These additional analyses are also included in Appendix A and have been recalculated to an anhydrous condition less MnO, P_2O_5, CO_2, and SO_4^{-2}. The inclusion of additional analyses from the John Day Formation creates a broader data base for comparisons on variation diagrams.

Silica values are high for samples JPW-101, JPW-157, JPW-207, JPW-230, JPW-277, JPW-283, and JPW-366. The author infers seconary SiO_2 may be responsible for the discrepancies. Hydrothermal precipitation of SiO_2 and devitrification processes could account for the additional silica.

The major oxides all show trends typical of a calc-alkaline series with increasing silica. Al_2O, TiO_2, CaO, FeO (total iron) and MgO all decrease and K_2O increases with increasing silica. The Na_2O plot gradually increases and then declines, for the author's analyses. This trend is similar to that illustrated by a Harker variation diagram for Lassen Peak, California (after Harker; in Bowen, 1928). The author also plotted CaO and $Na_2O + K_2O$ vs. SiO_2 on a Peacock diagram (1931). The resulting plot (Figure 34) yielded

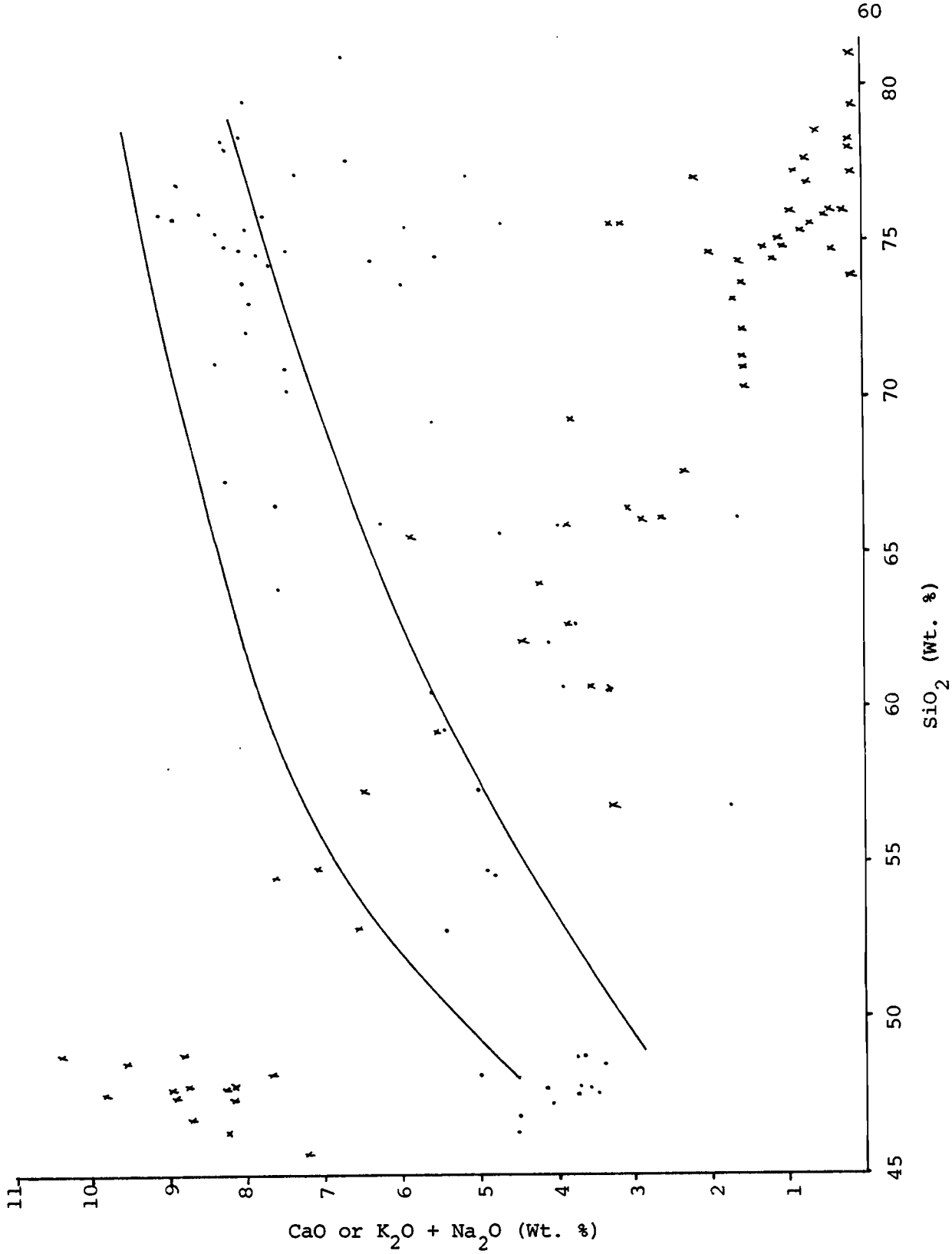

Figure 34. "Peacock Diagram" of John Day rocks. Dots represent K_2O + Na_2O vs. SiO_2. X's represent CaO vs. SiO_2. Solid lines represent Kuno's high-alumina basalt field.

an alkali-lime index of 58 indicating a calc-alkaline rock suite.

The author also compared the Na_2O/K_2O ratio (Figure 35) with Walker's (1970) variation diagram illustrating the slightly inverse relation of alkalies in Oregon ash-flow tuffs, some of which are from the John Day Formation. The author's plot of the geochemical analyses from Powell Buttes also results in a slightly inverse relationship of Na_2O/K_2O.

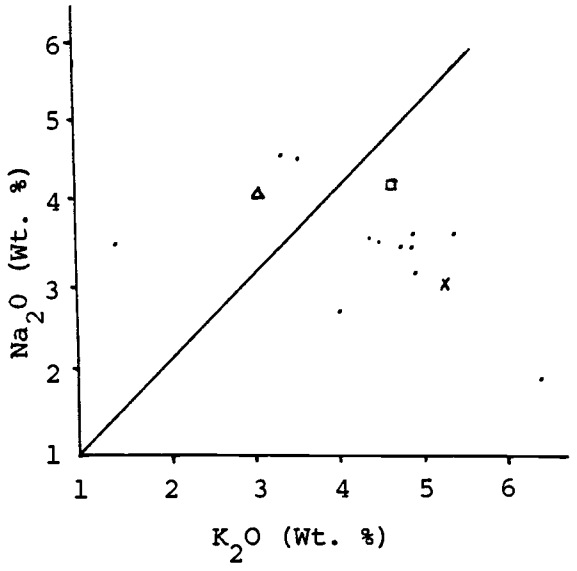

Figure 35. Variation diagram of Na_2O vs. K_2O (Weight %) illustrating the slightly inverse relationship of the alkalies. Δ - Average Rhyodacite, ▫ - Average Alkali Rhyolite, and x - Average Calc-alkaline Rhyolite, after Nockholds (1954).

GEOLOGIC HISTORY AND CONCLUSIONS

Powell Buttes represent a major silicic volcanic center of probable John Day age. The volcanic history evolved with the extrusion of extensive dacite flows. A few subordinate flows of basaltic andesite and one of rhyodacite were interbedded with the dacite. Through time, the lavas became progressively more silicic, and culminated in the deposition of large volumes of sparsely porphyritic flowbanded rhyolite. During the active stages of volcanism, many ash-flow tuffs were deposited and some of these underwent subsequent zeolitic diagenesis. The rhyolitic domes formed during the latter stages of volcanic activity at Powell Buttes, and faulting and tilting of the strata occurred after most of the rhyolite was deposited.

The author has associated Pelean type eruptions with the formation of the domes, ingnimbrites, and silicic lavas; Plinean type eruptions resulted in airfall tuffaceous sediments. The frequent volcanic ash falls are documented by fine-grained tuffs containing unidentifiable carbonized plant remains and former paleosoil horizons. Mineralogically, the tuffs of Powell Buttes resemble those of other tuffs of John Day age. At Powell Buttes, the crystal contents of the tuffs are estimated to range from a trace to 20 percent. Crystals observed in the tuffs include quartz, sanidine, oligoclase, and andesine and are similar to those noted by Peck (1961) and Swanson and Robinson (1968). The authigenic clinoptilolite noted at Powell Buttes has also been studied by Hay (1963) near Mitchell, Oregon. Chemically, the author's major-oxide analyses resemble other John Day major-oxide

analyses, with the exception the MgO is usually of such an insufficient quantity that it generally can not be recorded. On the basis of these observations, the author believes Powell Buttes was a source area for air-fall and ash-flow tuffs of John Day age.

Silicified wood was found as float and with the carbonized plant remains they indicate a semitropical climate with abundant foliage. Hodge (1942), Williams (1962), Hay (1963), and Baldwin (1976) have made similar observations.

Numerous periods of erosion occurred during the evolution of Powell Buttes and these relulted in erosional remnants such as Hat Rock and the deposition of epiclastic sediments. The erosional processes also contributed material to the Pliocene Deschutes Formation surrounding Powell Buttes and continued activity has resulted in the present day mature topography.

Hamilton and Meyers (1966), Hamilton (1969), Atwater (1970), and Lipman et al. (1972) hypothesize that a subduction zone existed off western North America during the early Tertiary. A later study by Rogers and Novitsky-Evans (1977) of the Clarno Formation in central Oregon suggested that a thin continental crust overlying a subducting plate, at a depth of approximately 120 km, was responsible for the calc-alkaline volcanism. Misyshiro (1974) has noted that with the advancing development of the continental-type crust above the subduction zone, the proportion of calc-alkaline rocks relative to all the volcanics tends to increase. Miyashiro also notes that there is a corresponding increase in the average SiO_2 percent of all the volcanic rocks. The author has noted a definite increase in silicic magmas with

the evolution of Powell Buttes, and plots of the geochemical analyses indicate a calc-alkaline suite.

The geothermal activity at Powell Buttes is significant since high geothermal gradients are usually not associated with old rhyolitic centers (Lachenbruch et al., 1975; MacLeod et al., 1977). The region surrounding Powell Buttes contains many other silicic centers that are probably of the same age and origin. Some of these centers include Bear Creek Butte 25 km southeast of Powell Buttes (Walker, 1977), Cline Buttes 22 km west-northwest of Powell Buttes (Peck 1961), and Grizzly Mountain 25 km north of Powell Buttes (Swanson, 1969 and Walker, 1977). Extensive flows and domes of rhyolite are also noted 30 km northwest of Powell Buttes (Peck, 1961) and 65 km north of Powell Buttes (Swanson, 1969 and Walker, 1977). Further investigations are needed to delineate the extent of this activity, determine the probable cause, the possible relation to the positive gravity anomaly of Pitts (1979), and the potential for broader utilization of this resource for purposes such as space heating.

REFERENCES CITED

Atwater, Tanya, 1970, Implications of Plate Tectonics for the Cenozoic Tectonic Evolution of Western North America: Geol. Soc. Am. Bull., V. 81, p. 3513-3536.

Baldwin, E. M., 1964, Geology of Oregon: Ann Arbor, Mich., Edwards Bros., Inc., 147 p.

Barnes, T. J., 1978, Geology of the Sand Mountain Area, Western Wheeler County, Oregon: Unpublished M.S. Thesis, Oregon State University, Corvallis, Oregon, 119 p.

Barrows, K. J., 1980, Zeolitization of Miocene Volcaniclastic Rocks Southern Desatoya Mountains, Nevada: Geol. Soc. Am. Bull., V. 91, Pt. 1, p. 199-210.

Bowen, N. L., 1928, The Evolution of the Igneous Rocks: New York, N. Y., Dover Publications, Inc., 332 p.

Calkins, F. C., 1902, A Contribution to the Petrography of the John Day Basin, Oregon: Calif. Univ. Pub. Dept. Geol. Bull., V. 3, p. 109-172.

Coleman, R. G., 1949, The John Day Formation in the Picture Gorge Quadrangle, Oregon: Unpublished M.S. Thesis, Oregon State University, Corvallis, Oregon, 211 p.

Couch, R., Gemperle, M., and Conrad, G., 1978, Total Field Aeromagnetic Anomaly Map, Cascade Mountain Range, Central Oregon: State of Oregon Dept. of Geol. and Min. Ind.

Davenport, R. E., 1971, Geology of the Rattlesnake and Older Ignimbrites in the Paulina Basin and Adjacent Area, Central Oregon: Unpublished PhD. Thesis, Oregon State University, Corvallis, Oregon, 132 p.

Deer, W. A., Howie, R. A., Zussman, J., 1966, An Introduction to the Rock Forming Minerals: London, Longman Group Ltd., 528 p.

Enlows, H. E., 1980, Personal Communication.

_____, 1976, Petrography of the Rattlesnake Formation at the Type Area, Central Oregon: State of Oregon Dept. of Geol. and Min. Ind. Short Paper 25, 34 p.

Evernden, J. F. and James, G. T., 1964, K/Ar Dates and Tertiary floras of North America: Am. Jour. Sci., V. 262, p. 945-974.

Evernden, J. F., Savage, D. E., James, G. H., and Curtis, G. H., 1964, K/Ar Dates and the Cenozoic Mammalian Chronology of North America Am. Jour. Sci., V. 262, p. 145-198.

Ewart, A., Hildreth, W., and Carmichael, I. S. E., 1975, Quaternary Acid Magma in New Zealand: Contrib. Min. and Petrol., V. 51, p. 1-27.

Fisher, R. V., 1967, Early Tertiary Deformation in North-central Oregon: Am. Assoc. Petrol. Geol. Bull., V. 51, No. 1, p. 111-123.

_____, 1966, Geology of a Miocene Ignimbrite Layer, John Day Formation: Calif. Univ. Pub. Geol. Sci., V. 67, 73 p.

_____, 1961, Proposed Classification of Volcaniclastic Sediments and Rocks: Geol. Soc. Am. Bull., V. 72, p. 1409-1414.

_____ and Wilcox, R. E., 1960, The John Day Formation in the Monument Quadrangle, Oregon: U. S. G. S. Prof. Paper 400-B p. 302-304

Goddard, R. L., 1970, Rock Color Chart: The Rock-Color Chart Committee, Geol. Soc. Am.

Goff, F. E., Donnelly, J. M., Thompson, J. M., 1977, Geothermal Prospecting in the Geysers - Clear Lake Area, Northern California: Geology, V. 5, No. 8, p. 509-515.

Hamilton, W. and Myers, W. B., 1966, Cenozoic Tectonics of the Western United States: Reviews of Geophysics, V. 4, No. 4, p. 509-549.

Hay R. L., 1978, Geologic Occurrence of Zeolites: in Natural Zeolites, Occurrence, Properties, and Use, Edited by L. B. Sand and F. A. Mumpton, New York, Pergamon Press, p. 135-143.

_____, 1963, Stratigraphy and Zeolitic Diagenesis of the John Day Formation of Oregon: Calif. Univ. Pub. Dept. Geol. Bull., V. 42, No. 5, p. 199-262.

_____, 1962, Soda-Rich Sanidine of Pyroclastic Origin From the John Day Formation of Oregon: The American Mineralogist, V. 47, p. 968-971.

_____, 1962, Origin and Diagenic Alteration of the Lower Part of the John Day Formation Near Mitchell, Oregon: Geol. Soc. Am., Buddington Memorial Memoir, p. 191-216.

_____ and Sheppard, R. A., 1977, Zeolites in Open Hydrologic Systems: in Mineralogy and Geology of Natural Zeolites, F. A. Mumpton, Editor, Mineralogical Society of America Short Course Notes, V. 4, p. 93-102.

Hodge, E. T., 1942, Geology of North Central Oregon: Oregon State College Studies in Geology, No. 3, 76 p.

_____, 1940, Geology of the Madras Quadrangle: Oregon State College, Studies in Geology, No. 1.

_____, 1932, New Evidence of the John Day Formation: Geol. Soc. Am. Bull., V. 43, p. 695-702.

Huggins, J. H., 1978, Geology of the Painted Hills Quadrangle, Wheeler County, North-central Oregon: Unpublished M.S. Thesis, Oregon State University, Corvallis, Oregon, 129 p.

Isherwood, W. F., 1976, Gravity and Magnetic Studies of the Geysers-Clear Lake Geothermal Region, Calif., U. S. A.: Second United Nations Symposium on the Development and Use of Geothermal Resources, San Francisco, Calif., V. 2, p. 1065-1073.

Jackson, K. C., 1970, Textbook of Lithology: San Francisco, McGraw-Hill Book Co., 552 p.

Johannsen, Albert, 1932a, A Descriptive Petrography of the Igneous Rocks: Chicago, University of Chicago Press, V. 1, 267 p.

_____, 1932b, A Descriptive Petrography of the Igneous Rocks: Chicago, University of Chicago Press, V. 2, 428 p.

Kerr, P. F. 1959, Optical Mineralogy: New York, McGraw-Hill Book Co., 442 p.

Kuno, H., 1968, Differentiation of Basaltic Magmas: in Basalts, V. 2, New York, Interscience Pub., p. 623-688.

Lachenbruch, A. H., Sass, J. H., Munroe, R. J. and Moses, T. H., Jr., 1976a, Geothermal Setting and Simple Heat Conduction Models for the Long Valley Caldera: Jour. Geophys. Research, V. 81, Pt. 1, p. 769-784.

_____, Sorrey, M. L., Lewis, R. E., Sass, J. H., 1976b, The Near-Surface Hydrothermal Regime of Long Valley, Calif.: Jour. Geophys. Research, V. 81, Pt. 1, p. 763-768.

Laniz, R. V., Stevens, R. E., Norman, M. B., 1964, Staining of Plagioclase Feldspar and other Minerals: U. S. G. S. Prof. Paper 501-B, p. 152-153.

Larsen, E. S., Jr., Gonyer, F. A., and Irving, J., 1937, Petrologic Results of a Study of the Minerals From the Tertiary Velcanic Rocks of San Juan Region, Colorado, 6. Biotite: American Mineralogist, V. 22, p. 898-905.

Laursen, J. M. and Hammond, Paul E., 1978, Summary of Radiometric Ages of Oregon Rocks Supplement I: July 1972 - December 1976: Isochron/West, No. 23, p. 3-28.

Lipman, P. W., Prostka, H. J., Christiansen, R. 1., 1972, Cenozoic Volcanism and Plate-tectonic Evolution of the Western United States, I. Early and Middle Cenozoic: Phil. Trans. Royal Soc. Lond., A. 271, p. 217-248.

Lofgren, Gary, 1971, Experimentally, Produced Devitrification Textures in Natural Rhyolitic Glass: Geol. Soc. Am. Bull., V. 82, p. 111-124.

MacLeod, N. S., Walker, G. S., McKee, E. H., 1977, Geothermal Significance of Eastward Increase in Age of Upper Cenozoic Rhyolitic Domes in Central Oregon: Second United Nations Symposium on Development and Use of Geothermal Resources, V. 1, p. 465-474.

McNitt, J. R., 1963, Exploration and Development of Geothermal Power in Calif.: Calif. Div. Mines and Geol. - Special Report 75, 44 p.

Marsch, O. C., 1875, Ancient Lake Basin in the Rocky Mountain Regions: Am. Jour. Science, Ser. 3, V. 9, p. 45-52.

Matthews, T. c., 1956, Radioactive Occurrences in Oregon: The Ore Bin - State of Oregon Dept. of Geol. and Mine. Ind., V. 18, No. 12, p. 105-107.

_____, 1955, Oregon Radioactive Discoveries in 1954 and 1955: The Ore Bin - State of Oregon Dept. of Geol. and Min. Ind., V. 17, No. 12, p. 87-92.

Merriam, J. C., 1901a, Geologic Section Through John Day Basin, (abs.): Geol. Soc. Am. Bull., V. 12, p. 496-497.

_____, 1901b, A Contribution to the Geology of the John Day Basin: Calif. Univ. Pub. Dept. Geol. Bull., V. 2, No. 9, p. 269-314.

Miyashiro, A., 1974, Volcanic Rock Series in Island Arcs and Active Continental Margins: Am. Jour. Sci., V. 274, p. 321-355.

Nockolds, S. R., 1954, Average Chemical Composition of Some Igneous Rocks: Geol. Soc. Am. Bull., V. 65, No. 10, p. 1007-1032.

_____, Knox, R. W. O'B., Chinner, B. A., 1978, Petrology for Students: New York, Cambridge University Press, 435 p.

Oles, K. F. and Enlows, H. E., 1971, Bedrock Geology of the Mitchell Quadrangle Wheeler County, Oregon: State of Oregon Dept. of Geol. and Min. Ind. Bull., 72, 62 p.

Peacock, M. A., 1931, Classification of Igneous Rock Series: Jour. Geol., V. 39, p. 54-67.

Peck, D. L., 1964, Geologic Reconnaissance of the Antelope-Ashwood Area north-central Oregon: U. S. G. S. Bull. 1161-D, 26 p.

_____, 1961, U. S. G. S. Geologic Map of Oregon West of the 121st Meridian, Scale 1:500,000.

Peterson, N. V., 1958, Oregon's Uranium Picture: The Ore Bin - State of Oregon Dept. of Geol. and Min. Ind., V. 20, No. 12, p. 111-117.

Pitts, G. S., 1979, Interpretation of Gravity Measurements Made in the Cascade Mountains and Adjoining Basin and Range Province in Central Oregon: Unpublished M.S. Thesis, Oregon State University, Corvallis, Oregon.

_____ and Couch, R., 1978, Complete Bouguer Gravity Anomaly Map - Cascade Mountain Range, Central Oregon: State of Oregon Dept. of Geol. and Min. Ind.

Robinson, P. t., 1969, High-Titania Alkali-Olivine Basalts of North-central Oregon, U. S. A.: Contrib. to Min. and Petrol., V.22, p. 349-360.

Rogers, J. J. W., 1966, Coincidence of Structural and Topographic Highs During Post-Clarno Time in North-Central Oregon: Am. Assoc. Petrol. Geol. Bull., V. 50, No. 2, p. 390-396.

_____ and Novitsky-Evans, J. M., 1977, The Clarno Formation of Central Oregon, U. S. A. -- Volcanism on a Thin Continental Margin: Earth and Planetary Science Letters, V. 34, p. 55-56.

Ross, C. S. and Smith, R. L., 1960, Ash-Flow Tuffs - Their Origin, Geologic Relations, and Identification: U. S. G. S. Prof. Paper 366, 81 p.

Russell, I. C., 1905, Preliminary Report on the Geology and WAter Resources of Central Oregon: U. S. G. S. Bull. 252, 138 p.

Schafer, M., 1956, Uranium Prospecting in Oregon in 1956: The Ore Bin - State of Oregon Dept. of Geol. and Min. Ind., V. 18, No. 12, p. 101-104.

Smith, R. 1., 1960, Ash-Flows: Geol. Soc. Am. Bull., V. 71, Pt. 2, p. 795-841.

Streckeisen, A. 1979, Classification and Nomenclature of Volcanic Rocks, Lamprophyres, Carbonaties, and Melilitic Rock: Recommendations and Suggestions of the I. U. G. S. Subcommission on the Systematics of Igneous Rocks: Geology, V. 7, p. 331-335.

Stroh, H. R., 1980, Geology of the Clarno Formation in the Vicinity of Stephenson Mountain, Jefferson, Crook, and Wheeler Counties, Oregon: Unpublished M. S. Thesis, Oregon State University, Corvallis, Oregon, 128 p.

Swanson, D. A., 1969, Reconnaissance Geologic Map of the East Half of Bend Quadrangle, Crook, Wheeler, Jefferson, Wasco, and Deschutes Counties, Oregon: U. S. G. S. Map I-568.

_____ and Robinson, P. T., 1968, Base of the John Day Formation in and near the Horse Heaven Mining District, North-Central Oregon: U. S. G. S. Prof. Paper 600-D, p. D154-D161.

Taylor, E. M., 1980a, Personal Communication.

_____, 1980b, High Cascade Ash-flow tuffs and Pumice Deposits in the Vicinity of Bend Oregon: Abstracts with Programs, Cordilleran Section, Geol. Soc. Am., V. 12, No. 3, p. 155.

_____, 1978, Field Geology of S. W. Broken Top Quadrangle, Oregon: State of Oregon Dept. of Geol. and Min. Ind. Bull., Special Paper No. 2.

_____, 1960, Geology of the Clarno Basin Mitchell Quadrangle, Oregon: Unpublished M. S. Thesis, Oregon State University, Corvallis, Oregon, 173 p.

Vance, J. A., 1965, Zoning in Igneous Plagioclase and Patchy Zoning: Jour. Geol., V. 73, p. 636-651.

_____, 1962, Zoning in Igneous Plagioclase: Normal and Oscillatory Zoning: Am. Jour. Science, V. 260, p. 746-760.

Walker, G. W., 1977, U. S. G. S. Geologic Map of Oregon East of the 121st Meridian, two sheets, Scale 1:500,000.

_____, 1970, Cenozoic Ash-flow tuffs of Oregon: The Ore Bin - State of Oregon Dept. of Geol. and Min. Ind. Bull., B. 32, p. 97-115.

_____, Cox, A., Doell, R. R., Gromme, C. S., 1967, Pliocene Geomagnetic Epochs: Earth and Planetary Science Letters, V. 2, p. 163-173.

Walker, G. W., Dalrymple, G. B., Lanphere, M. A., 1974, Index to K/Ar Dates of Cenozoic Volcanic Rocks of Oregon: U. S. G. S. Misc. Field Studies Map MF-569.

Waters, A. C., 1968, Reconnaissance Geologic Map of the Madras Quadrangle, Jefferson, and Wasco, Counties, Oregon: U. S. G. S. Misc. Geol. Inv. Map I-555, Scale 1:125,000.

_____, 1954, John Day Formation West of its Type Locality (abs.): Geol. Soc. Am. Bull., V. 65, Pt. 2, p. 1320.

Wells, F. G. and Peck, D. L., 1961, Geologic Map of Oregon West of the 121st Meridian: U. S. G. S. Misc. Geol. Inv. Map I-325, Scale: 1:500,000.

Williams, H. 1962, The Ancient Volcanoes of Oregon: Condon Lectures - Oregon State System of Higher Education, 55 p.

_____, 1957, A Geologic Map of the Bend Quadrangle, Oregon and a Reconnaissance Geologic Map of the Central Portion of the High Cascade Mountains: State of Oregon Dept. of Geol. and Min. Ind., Map and Text.

Winchell, A. N., 1951, Elements of Optical Mineralogy: New York, John Wiley and Sons, Inc., 551 p.

APPENDICES

Appendix A: Chemical Analyses of John Day Rocks. (Major oxides tabulated are in weight percent.) Sources: Hay (1962), Hay (1963), Peck (1964), Fisher (1966), Swanson and Robinson (1968), Robinson (1969), Oles and Enlows (1971), and Weidenheim (this study).

Chemical Analyses
Hay (1963)

Sample	1	2	3	4	5	6
SiO_2	75.23	74.86	75.42	76.86	74.82	75.50
TiO_2	0.32	0.32	0.39	0.45	0.26	0.97
Al_2O_3	12.20	12.57	13.10	12.77	14.09	11.35
FeO*	2.95	2.97	2.21	0.34	2.52	2.71
MgO	0.18	0.29	0.25	0.06	0.13	0.42
CaO	0.75	0.96	0.68	0.67	0.37	3.12
Na_2O	3.26	3.81	3.99	2.79	4.47	2.76
K_2O	5.11	4.22	3.96	6.06	3.34	3.16
Total	100.00	100.00	100.00	100.00	100.00	100.00

1 Black densely welded vitric tuff, from basal 25 ft. thick flow unit of ignimbrite in center N½, SW¼, Sec. 31, T. 10 S., R. 21 E.

2 Pale-gray densely welded vitric tuff, seven feet above base of ignimbrite near SW Cor. Sec. 1, T. 10 S., R. 22 E.

3 Yellowish-gray devitirfied densely welded tuff, six feet above base of a 40 ft. unit of welded tuff in NW¼, SW¼, Sec. 31, T. 10 S., R. 21 E.

4 Very light gray semiwelded devitrified tuff, three feet above base of a 15 ft. unit of devitrified tuff forming a hogback in NW¼, NE¼, Sec. 36, T. 10 S., R. 20 E.

5 Pale yellowish-brown devitrified glass, from 5-10 feet above base of claystone overlying a 40 ft. thick massive devitrified welded tuff in center S line NW¼, Sec. 31, T. 10 S., R. 21 E.

6 Yellowish-gray thick-walled zeolitized pumice fragment, 25-30 ft. above exposed base of ignimbrite in center NE¼, Sec. 36, T. 10 S. R. 20 E.

Chemical Analyses
Hay (1963)

Sample	7	8	9	10	11	12
SiO_2	74.46	65.73	65.90	63.84	65.91	65.40
TiO_2	0.47	1.40	0.51	0.73	1.31	1.23
Al_2O_3	12.40	12.41	19.06	10.94	13.51	12.72
FeO*	3.86	10.34	6.87	11.23	9.02	8.47
MgO	0.79	2.33	3.19	1.50	1.30	1.59
CaO	1.65	3.84	2.83	4.19	2.67	5.84
Na_2O	1.45	2.01	1.16	2.02	2.49	1.47
K_2O	4.93	1.95	0.49	5.54	3.78	3.27
Total	100.01	100.01	100.01	99.99	99.99	99.99

7 Grayish-yellow zeolitized ignimbrite, from 15 ft. above exposed base of ignimbrite at same locality as no.6.

8 Dusky-yellow zeolitic claystone, from ignimbrite about 35 ft. below a layer of welded tuff in center SW¼, Sec. 33, T. 10 S., R. 21 E.

9 Dusky yellowish-green zeolitized ignimbrite, from 5 ft. of altered ignimbrite underlying devitrified welded tuff in center N½, SW¼, Sec. 31, T. 10 S., T. 21 E.

10 Grayish-green pumice, from centers of celadonitic concretions collected 30-50 ft. above base of ignimbrite in center S edge NW¼, Sec. 22, T. 10 S., R. 22 E.

11 Dusky yellowish-green zeolitized ignimbrite, from same location as no. 10.

12 Dusky yellowish-green zeolitized ignimbrite, from 90-100 ft. above base of ignimbrite in center S½, SW¼, Sec. 1, T. 10 S., R. 22 E.

Chemical Analyses
Hay (1963)

Sample	13	14	15	16	17	18
SiO_2	73.52	74.68	68.23	77.01	60.54	60.62
TiO_2	0.50	0.61	0.92	0.61	2.11	1.35
Al_2O_3	13.43	13.23	14.02	12.44	19.54	22.24
FeO*	4.14	3.29	6.13	1.87	7.93	6.85
MgO	0.94	0.69	1.39	0.47	1.01	1.45
CaO	1.52	1.99	3.77	2.16	3.29	3.51
Na_2O	1.88	2.37	2.58	1.79	1.63	3.39
K_2O	4.07	3.15	2.96	3.63	3.96	0.58
Total	100.00	100.01	100.00	99.98	100.01	99.99

13 Yellowish-gray coarse vitric tuff, from 65 ft. unit of medium- to coarse-grained tuff about 200 ft. below ignimbrite in NE¼, SE¼, Sec. 13, T. 10 S., R. 20 E.

14 Yellowish-gray zeolitized tuff, from 45 ft. unit of medium- to coarse grained tuff about 215 feet below ignimbrite in NW¼, SW¼, Sec. 31, T. 10 S., R. 21 E.

15 Grayish-green zeolitized tuff, from medium- and coarse grained tuff 150-170 ft. below ignimbrite in center S½, SW¼, Sec. 22, T. 10 S., R. 21 E.

16 White fine-grained zeolitized tuff, about 170 ft. above base of formation in center N edge NE Cor. Sec. 1, T. 11 S., R. 20 E.

17 Dusky yellow claystone, collected 65 ft. above base of formation near SW Cor. Sec. 36, T. 10 S., R. 20 E.

18 Pale yellowish-green claystone, from approximately 250 ft. above base of formation at E edge NE¼, Sec. 1, T. 11 S., R. 20 E.

Chemical Analyses
Hay (1963)

Sample	19	20
SiO_2	62.56	62.00
TiO_2	1.30	1.53
Al_2O_3	16.01	15.01
FeO*	10.72	10.64
MgO	1.86	2.32
CaO	3.84	4.48
Na_2O	1.85	2.22
K_2O	1.87	1.81
Total	100.01	100.01

19 Dusky-yellow claystone, collected 165 ft. below ignimbrite in NW¼, SW¼, Sec. 31, T. 10 S., R. 21 E.

20 Dusky-yellow claystone, collected 80 ft. above ignimbrite near NW Cor. Sec. 36, T. 10 S., R. 20 E.

Chemical Analyses
Peck (1964)

Sample	DLP 58-42	DLP 58-32	DLP 58-50	5	DLP 58-39A
SiO_2	75.73	74.87	77.03	75.92	77.58
TiO_2	0.17	0.31	0.19	0.04	0.17
Al_2O_3	13.71	12.57	11.90	13.65	12.25
FeO*	1.65	3.56	2.67	0.83	2.21
MgO	0.13	---	0.10	0.07	0.35
CaO	0.92	1.26	0.81	0.38	0.66
Na_2O	2.43	4.08	2.30	4.67	3.12
K_2O	5.27	3.35	5.01	4.43	3.65
Total	100.01	100.00	100.01	99.99	99.99

DLP58-42 Welded tuff; from vitric base of ash-flow sheet of member A in Sec. 12, T. 10 S., R. 16 E. at 3350 ft. elevation on bank of county road 1.9 miles S. 62 W. of Ashwood.

DLP58-32 Trachyandesite; from flow of member B in Sec. 10, T. 10 S., R. 16 E. at 3725 ft. elevation on bank of county road 2.6 miles S. 61 W. of Ashwood.

DLP58-50 Welded tuff; from vitric base of ash-flow sheet of member E in Sec. 18, T. 8 S., R. 17 E., on bank of county road 2.6 miles S. 25 W. of Antelope.

5 Rhyolite from near Antelope.

DLP58-39A Welded tuff from vitric base of welded ash-flow sheet of member H in Sec. 20. T. 9 S., R. 15 E. in roadcut on east side of former U. S. Highway 97, one-half mile south of Pacific States Cut Stone Quarry.

Chemical Analyses
Fisher (1966)

Sample	62-137	62-376
SiO_2	72.91	74.28
TiO_2	0.22	0.21
Al_2O_3	14.14	13.13
FeO*	3.10	3.09
MgO	0.07	0.09
CaO	1.64	1.53
Na_2O	3.89	4.05
K_2O	4.04	3.62
Total	100.01	100.00

62-137 Vitrophyre.

62-376 Vitrophyre.

Chemical Analyses
Swanson and Robinson (1968)

Sample	DAS 66-208	DAS 66-90
SiO_2	78.42	74.95
TiO_2	0.20	0.53
Al_2O_3	12.36	13.78
FeO*	0.25	1.27
MgO	0.12	0.21
CaO	0.58	1.03
Na_2O	2.55	2.57
K_2O	5.51	5.65
Total	99.99	99.99

DAS66-208 Porphyritic welded tuff; member A, roadcut along county road 2.2 miles southwest of Ashwood, NE¼, NE¼, Sec. 10, T. 10 S., R. 16 E.

DAS 66-90 Porphyritic Welded tuff; east side of Opal Mountain, SW¼, NW¼, Sec. 36, T. 11s., R. 18 E.

Chemical Analyses
Robinson (1969)

Sample	3	4	5	6	7	8
SiO_2	46.74	47.59	47.20	48.40	48.69	47.66
TiO_2	4.21	3.69	4.21	3.13	2.83	3.63
Al_2O_3	15.21	14.92	14.46	15.88	15.53	15.56
FeO*	16.34	15.40	16.88	13.63	13.92	15.44
MgO	4.35	5.94	5.03	6.03	6.60	5.16
CaO	8.67	8.76	8.14	9.55	8.77	8.96
Na_2O	3.66	2.80	3.05	2.7	2.82	2.82
K_2O	0.83	0.90	1.02	0.68	0.83	0.76
Total	100.01	100.00	99.99	100.00	99.99	99.99

3 Olivine basalt, member E, 1.3 miles southwest of Antelope, Oregon, SE¼, SW¼, Sec. 6, T. 8 S., R. 17 E.

4 Olivine basalt, member E., 7.5 miles southwest of Antelope, Oregon, NE¼, SW¼, Sec. 6, T. 8 S., R. 17 E.

5 Olivine basalt, member F., 3.6 miles southwest of Antelope, Oregon, SE¼, SW¼, Sec. 15, T. 8 S., R. 17 E.

6 Olivine basalt, member F., lowest flow, 4.5 miles east of Antelope, Oregon, SW¼, SE¼, Sec. 36, T. 7 S., R. 17 E.

7 Olivine basalt, member F., middle flow, 4.5 miles east of Antelope, Oregon, SW¼, SE¼, Sec. 36, T. 7 S., R. 17 E.

8 Olivine basalt, member F., upper flow 4.5 miles east of Antelope, Oregon, SW¼, SE¼, Sec. 36, T. 7 S., R. 17 E.

Chemical Analyses
Robinson (1969)

Sample	9	10	11	12	13	14
SiO_2	47.45	46.15	47.63	48.64	47.40	45.33
TiO_2	3.77	4.04	3.86	2.78	2.88	4.78
Al_2O_3	15.06	14.82	15.05	17.00	16.68	16.51
FeO*	15.96	17.47	16.39	13.89	13.34	17.29
MgO	5.37	4.82	4.73	3.64	6.2	2.82
CaO	8.92	8.19	8.21	10.33	9.76	7.21
Na_2O	2.81	3.57	3.12	3.04	3.28	4.19
K_2O	0.66	0.95	1.01	0.68	0.46	1.87
Total	100.00	100.01	100.00	100.00	100.00	100.00

9 Olivine basalt, member F., 5.4 miles northeast of Clarno, Oregon, NE¼, NE¼, Sec. 13, T. 7 S., R. 19 E.

10 Olivine basalt, member F., Road cut 7.3 miles southsest of Antelope, Oregon, NW¼, SW¼, Sec. 22, T. 8 S., R. 16 E.

11 Olivine basalt, member F., 0.5 miles west of Antelope, Oregon, SW¼, SW¼, Sec. 31, T. 7 S., R. 17 E.

12 Olivine basalt, member H(?), 3.8 miles northwest of Kinzua, Oregon, SW¼, SW¼, Sec. 15, T. 6 S., R. 22 E.

13 Olivine basalt, member H(?), 3.5 miles northwest of Kinzua, Oregon, SW¼, SW¼, Sec. 21, T. 6 S., R. 22 E.

14 Olivine basalt, lower member, 3 miles northwest of Twickenham, Oregon, SE¼, NE¼, Sec. 32, T. 9 S., R. 21 E.

Chemical Analyses
Robinson (1969)

Sample	15	16	17	18	19	20
SiO_2	48.11	59.21	54.73	57.16	52.71	70.19
TiO_2	3.35	1.76	2.89	1.88	3.02	0.55
Al_2O_3	15.38	14.28	14.07	13.79	15.19	13.62
FeO*	15.81	12.00	13.50	13.69	14.33	6.61
MgO	4.72	1.72	2.79	1.99	2.71	0.08
CaO	7.63	5.55	7.08	6.48	6.64	1.49
Na_2O	3.51	3.81	3.36	2.93	3.71	3.86
K_2O	1.47	1.68	1.58	2.09	1.69	3.60
Total	99.98	100.01	100.00	100.01	100.00	100.00

15 Olivine basalt, lower member, near northwest corner section 9, T. 10 S., R. 21 E.

16 Trachyandesite, member B, 3.5 miles northeast of Clarno, Oregon, between NW¼, and NE¼, SE¼, Sec. 23, T. 7 S., R. 19 E.

17 Trachyandesite, member B, 4 miles south of Antelope, Oregon, SE¼, SE¼, Sec. 20, T. 8 S., R. 17 E.

18 Trachyandesite, member B. 2.6 miles south 61° west of Ashwood, Oregon, Sec. 10, T. 10 S., R. 16 E.

19 Trachyandesite, member H(?), 2.25 miles northeast of Fossil, Oregon, SW¼, SE¼, Sec. 22, T. 6 S., R. 21 E.

20 Quartz latite, member H(?), 1.5 miles northeast of Fossil, Oregon, NW¼, SE¼, Sec. 30, T. 6 S., R. 21 E.

Chemical Analyses
Robinson (1969)

Sample	21
SiO_2	70.91
TiO_2	0.51
Al_2O_3	13.92
FeO*	5.44
MgO	0.12
CaO	1.63
Na_2O	3.81
K_2O	3.65
Total	99.99

21 Quartz latite, member H(?), 2 miles northeast of Fossil, Oregon, SW¼, NE¼, Sec. 27, T. 6 S., R. 21 E.

Chemical Analyses
Oles and Enlows (1971)

Sample	Mitchell Sample No. 1
SiO_2	71.00
TiO_2	0.48
Al_2O_3	13.40
FeO*	5.00
MgO	0.30
CaO	1.50
Na_2O	4.35
K_2O	3.96
Total	99.99

No. 1 Ignimbrite.

Chemical Analyses
Weidenheim (1980)

Sample	JPW-36	JPW-101	JPW-117	JPW-134	JPW-157	JPW-168
SiO_2	72.0	78.7	75.9	67.5	78.0	66.2
TiO_2	0.35	0.10	0.25	0.80	0.30	0.80
Al_2O_3	14.0	11.0	11.4	15.53	9.8	15.5
FeO*	3.0	2.3	3.4	5.0	4.0	4.1
MgO	---	---	---	0.30	---	1.8
CaO	1.5	0.10	0.20	2.3	0.10	3.32
Na_2O	4.6	3.6	3.6	4.1	3.5	4.3
K_2O	3.35 ~~0.35~~	4.40 ~~0.10~~	4.95 ~~0.25~~	3.92 ~~0.80~~	4.75 ~~0.30~~	3.54
Total	98.80	100.20	99.70	99.45	100.45	99.65

JPW-36 Porphyritic augite-bearing rhyodacite: elevation 4420 ft., NE¼, SE¼, Sec. 13, T. 16 S., R. 14 E.

JPW-101 Porphyritic flowbanded rhyolite: elevation 3640 ft., NW¼, SW¼, Sec. 32, T. 15 S., R. 15 E.

JPW-117 Porphyritic rhyolite: elevation 4780 ft., SE¼, NE¼, Sec. 7, T. 16 S., R. 15 E.

JPW-134 Porphyritic dacite: elevation 4040 ft., SW¼, NW¼, Sec. 16, T. 16 S., R. 15 E.

JPW-157 Porphyritic flowbanded rhyolite: elevation 4750 ft., SE¼, SW¼, Sec. 13, T. 16 S., R. 14 E.

JPW-168 Two-pyroxene dacite: elevation 3945 ft., NE¼, NE¼, Sec. 23, T. 16 S., R. 14 E.

The weight percentages were determined within the following limits:

FeO	0.1	SiO_2	0.2
TiO_2	0.05	Al_2O_3	0.3
CaO	0.1	Na_2O	0.1
K_2O	0.05	MgO	0.1

Chemical Analyses
Weidenheim (1980)

Sample	JPW-176	JPW-207	JPW-230	JPW-277	JPW-283	JPW-366
SiO_2	54.5	77.2	81.0	78.3	79.4	75.8
TiO_2	2.0	0.30	0.20	0.15	0.15	0.30
Al_2O_3	15.5	9.8	10.7	11.3	11.1	9.8
FeO*	10.6	4.5	1.1	2.4	1.8	5.7
MgO	4.2	---	---	---	---	---
CaO	7.6	0.10	0.10	0.10	0.10	0.04
Na_2O	3.5	3.2	2.7	3.5	3.5	3.6
K_2O	1.3	5.0	4.05	4.80	4.50	5.30
Total	99.40	100.10	99.85	100.35	100.55	100.90

JPW-176 Porphyritic augite-bearing basaltic andesite: elevation 4240 ft., NE¼, NE¼, Sec. 24, T. 16 S., R. 14 E.

JPW-207 Porphyritic flowbanded rhyolite: elevation 4100 ft., SW¼, NW¼, Sec. 6, T. 16 S., R. 15 E.

JPW-230 Porphyritic rhyolite: elevation 4210 ft., SW¼, NW¼, Sec. 6, T. 16 S., R. 15 E.

JPW-277 Porphyritic rhyolite: elevation 3760 ft., SE¼, SW¼, Sec. 32, T. 15 S., R. 15 E.

JPW-283 Microspherulitic rhyolite: elevation 4630 ft., SW¼, SW¼, Sec. 5, T. 16 S., R. 15 E.

JPW-366 Porphyritic rhyolite: elevation 3630 ft., SW¼, NW¼, Sec. 15, T. 16 S., R. 15 E.

Appendix B: SiO_2 Variation Diagrams of Selected John Day Rocks. (Points plotted are from analyses tabulated in Appendix A.)

Sources of analyses:

+ Hay (1962)
⊤ Hay (1963)
∘ Peck (1964)
□ Fisher (1966)
⊥ Swanson and Robinson (1968)
× Robinson (1969)
Δ Oles and Enlows (1971)
· Weidenheim (this study)

Note: $FeO^* = Fe_2O_3 + FeO$

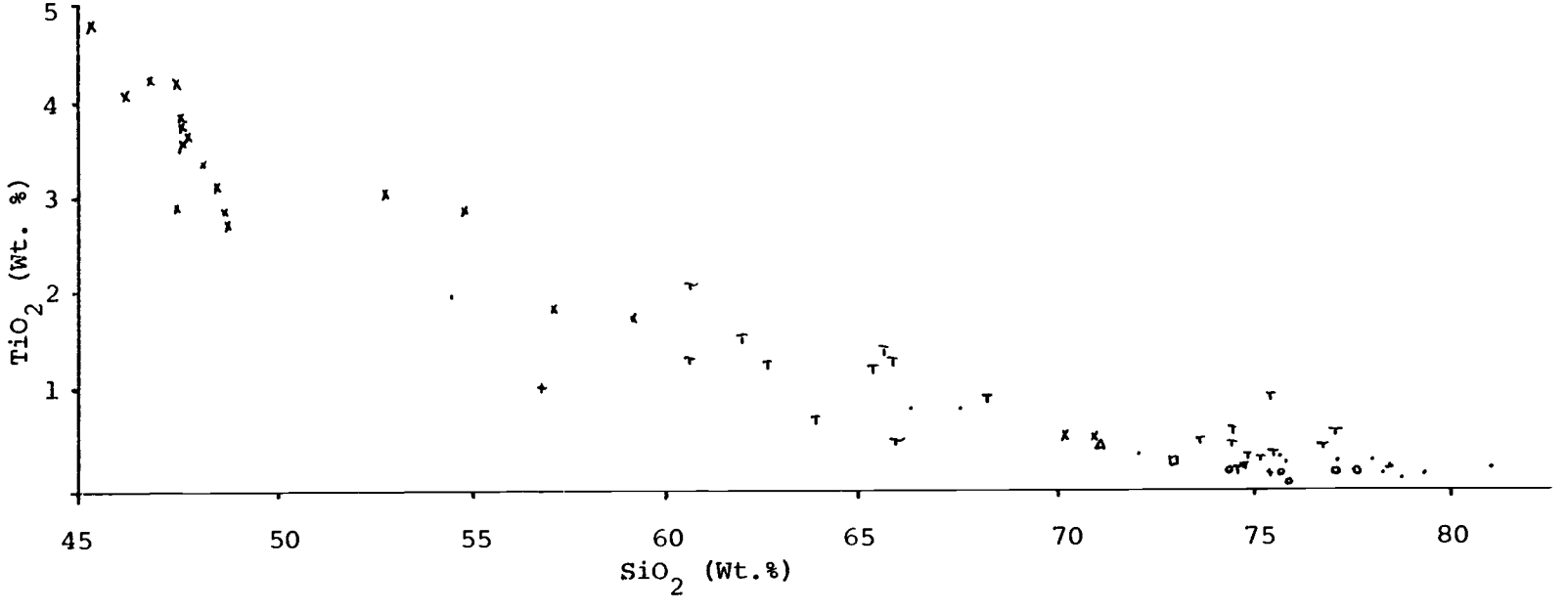
5
4
3
2
1
TiO_2 (Wt. %)
45
50
55
60
65
70
75
80
SiO_2 (Wt.%)

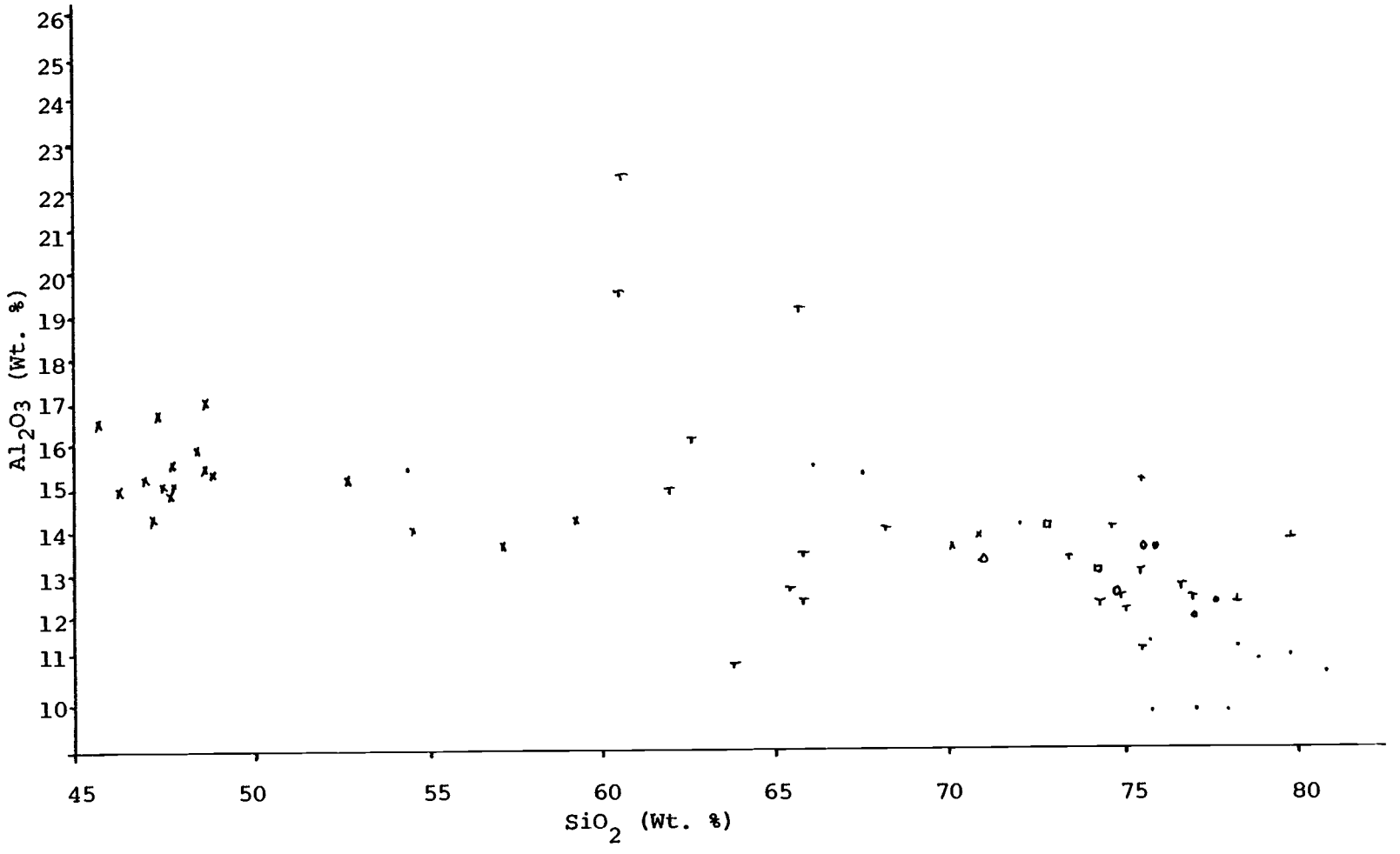
26
25
24
23
22
21
20
19
18
17
16
15
14
13
12
11
10
Al_2O_3 (Wt. %)
45
50
55
60
65
70
75
80
SiO_2 (Wt. %)

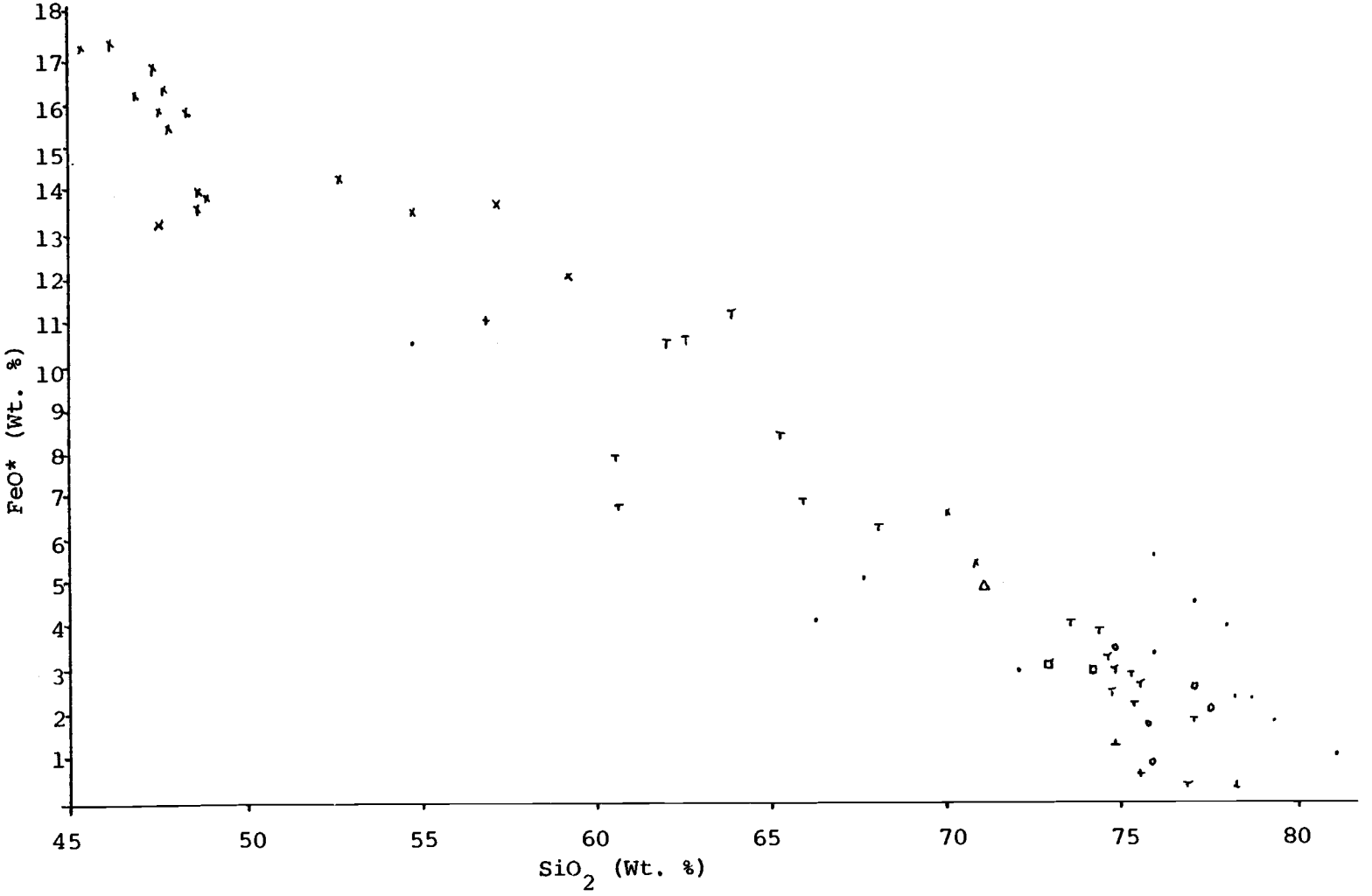
FeO* (Wt. %)
18
17
16
15
14
13
12
11
10
9
8
7
6
5
4
3
2
1
45
50
55
60
65
70
75
80
SiO2 (Wt. %)

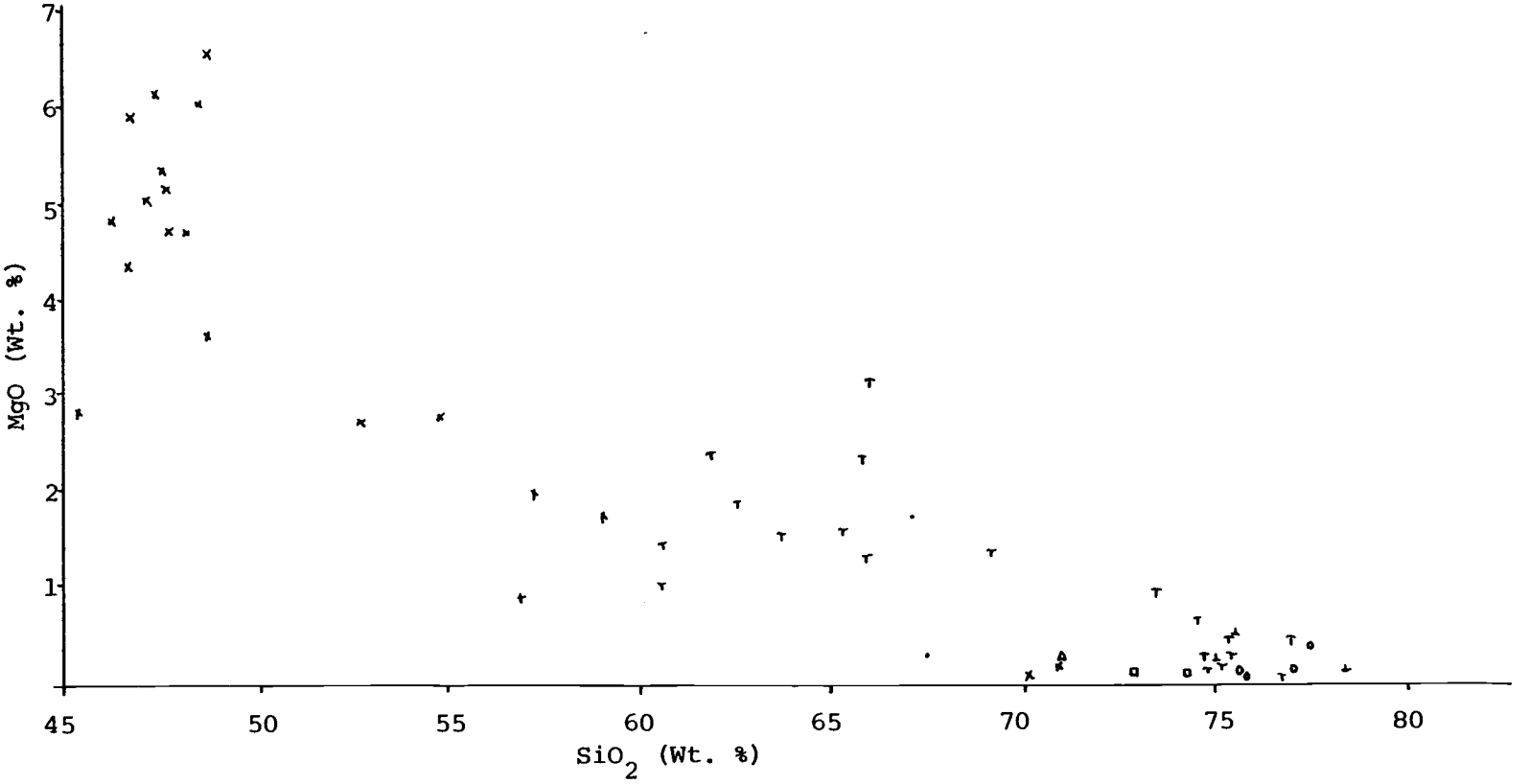
MgO (Wt. %)
7
6
5
4
3
2
1
45
50
55
60
65
70
75
80
SiO2 (Wt. %)

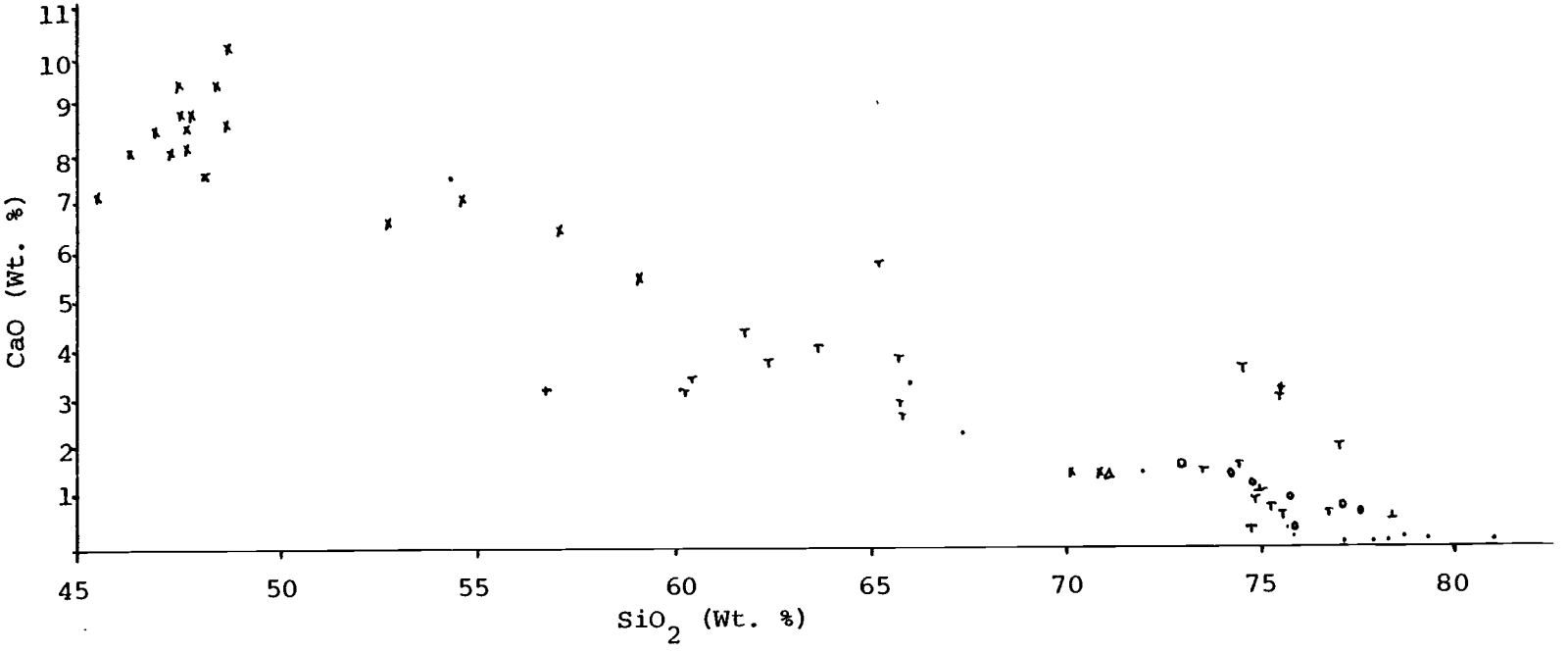
CaO (Wt. %)
11
10
9
8
7
6
5
4
3
2
1
45
50
55
60
65
70
75
80
SiO2 (Wt. %)

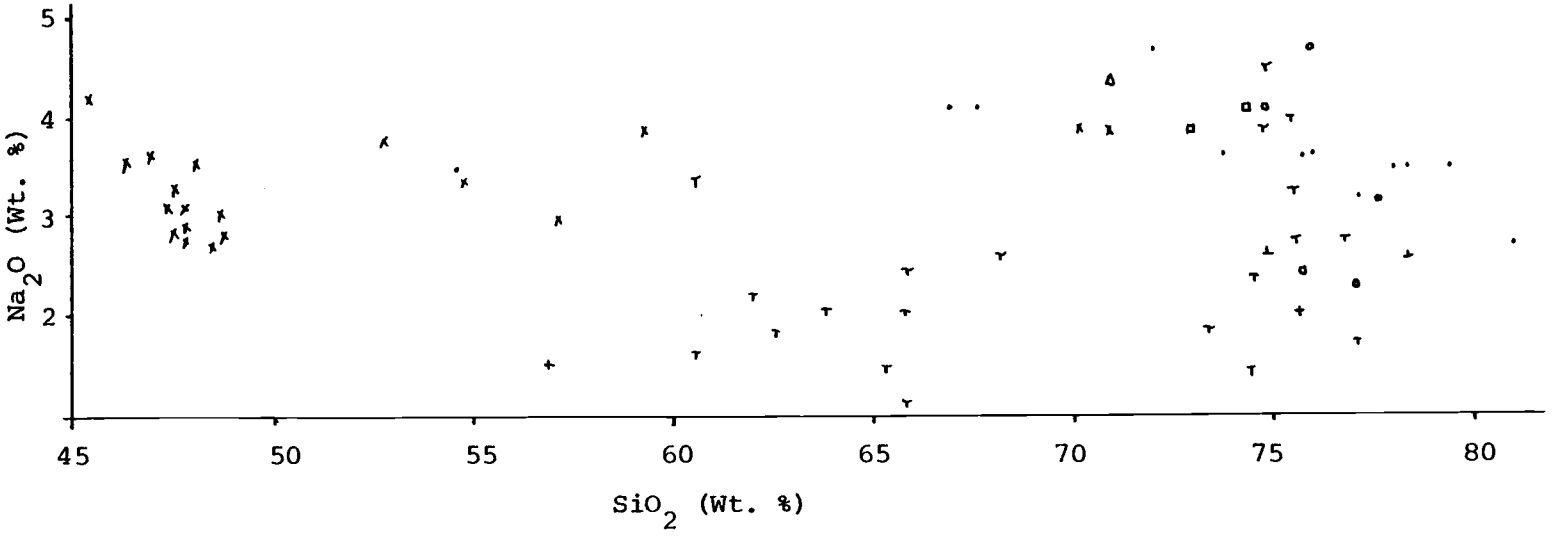
5
4
3
2
Na_2O (Wt. %)
45
50
55
60
65
70
75
80
SiO_2 (Wt. %)

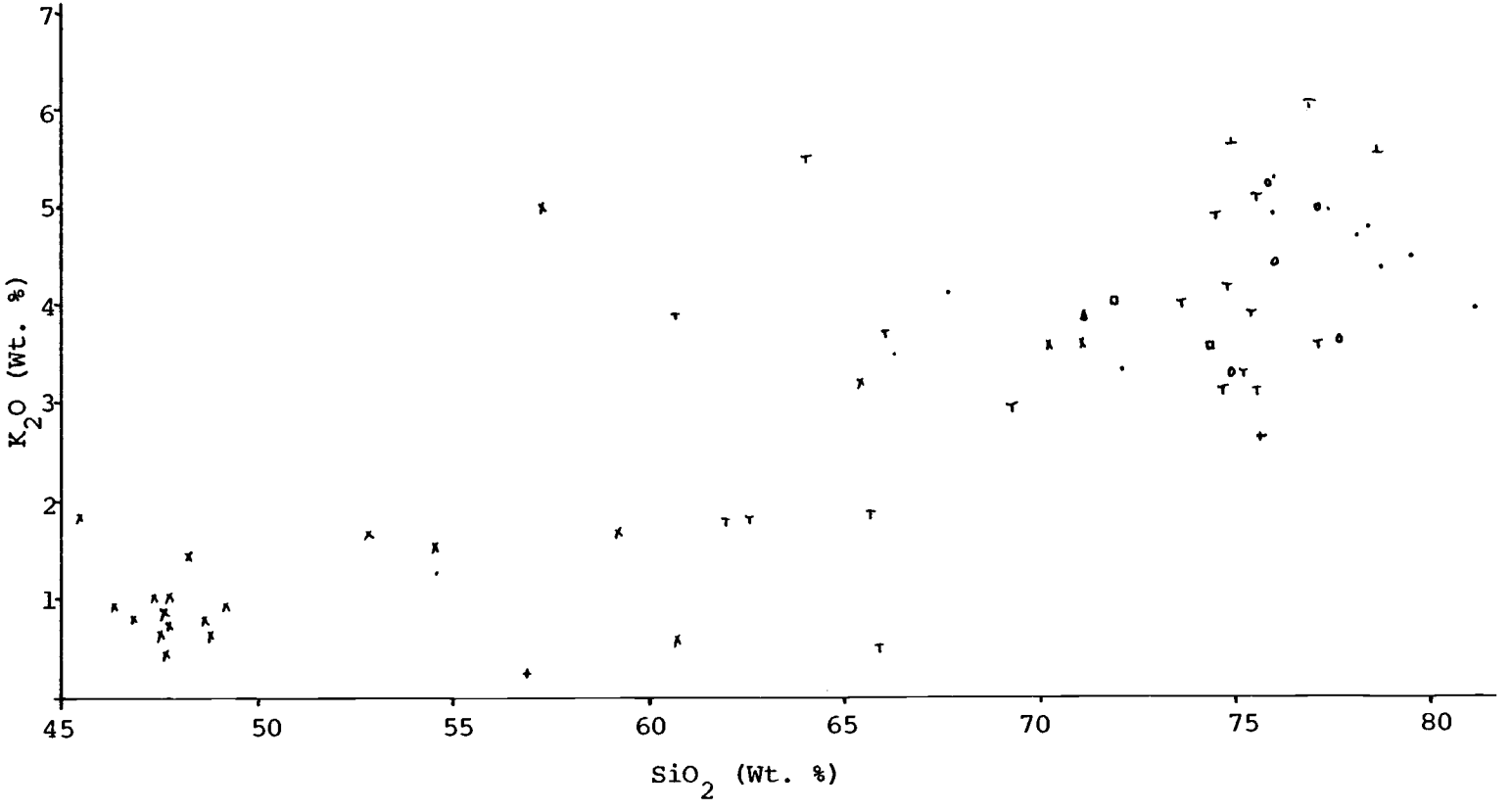
7
6
5
4
3
2
1
K_2O (Wt. %)
45
50
55
60
65
70
75
80
SiO_2 (Wt. %)